UNIVERSITY OF BIRMINGHAM

DEPARTMENT OF

METALLURGY AND MATERIALS

UNIVERSITY OF
BIRMINGHAM

Master of Research in Science and Engineering of Materials 2010-2011

THESIS

Processing and characterization of liquid crystal nanocomposites

by

Chung Ka Fai (1043058)

February 2013

Processing and characterization of liquid crystal nanocomposites

by

Chung Ka Fai (1043058)

Submitted in partial fulfillment of the

Requirements for the degree of

MASTER OF RESEARCH

IN

SCIENCE AND ENGINEERING OF MATERIALS

From

University of Birmingham

February 2013

Project supervisors: Dr. ITH Chang & Dr. SN Kukureka

Table of contents

List of figures

List of tables

Page

Acknowledgement

I would like to thank my supervisors, Dr. ITH Chang & Dr. SN Kukureka, for giving me an opportunity to study the topic of LC nanocomposites, their guidance and support. Both of them gave me valuable advices and ideas during the whole project period. I appreciated their contributions and hard work.

I would also like to thank Professor Tim Button, Dr. Martin Strangwood, Dr. Clive Ponton, Dr. Jacqueline Deans, Mr. Frank Biddlestone, Mr. Paul Stanley, Mr. Karl Megg and Miss. Elaine Mitchell for technical and equipment supports.

As an international student for only one year, I cherished the moment in the University of Birmingham. I enjoyed the school campus and working with people in the Metallurgy and Materials department and rest of the university.

Abstract

Due to the increased popularity of fast response display, the driving force to make high-speed switching liquid crystal (LC) material is raised. Doping nanoparticles such as carbon nanotubes (CNTs) in LC material is one of the methods to improve the display performance. Recently, many studies reported that enhancement of electro-optical (EO) performance was achieved by LC nanocomposites. The attraction of the hybrid system is not only the advance in EO performance, but also the alignment of CNTs. The disordered nature of CNTs makes it hard to expose the excellent properties and the self-ordered nature of LC material perfectly fit in this problem. Moreover, with LC acts as host, the CNTs orientation can be manipulated by external electric or magnetic field. This creates a promising future for novel nano-devices. On the other hand, there are doubts or questions on the stability of the nanocomposites and optimization of the sonication parameters and CNTs concentration that needed to be addressed before the mass production in the industry.

In this thesis, liquid crystal material 5CB and multi-walled carbon nanotubes (MWCNTs) hybrid system was studied. Normally white (NW) mode of liquid crystal cells were fabricated and the EO performance and the dispersion effectiveness were investigated.
The measured results revealed that small amount of anisotropic MWCNTs incorporated well with 5CB. This modifies the dielectric anisotropy and the viscosity of the mixture, thereby changing the threshold voltage and the switching behavior of a liquid crystal device.

In order to obtain an improvement of the EO performance, a uniform dispersion is critical and it is highly depends on the applied energy (either stirring or sonication or both), time, temperature and the concentration of CNTs. Results showed that the fastest response time of the nanocomposite was achieved in the following conditions: 1. Short sonication time (5mins)

with prior stirring. 2. Sonication under ice bath. 3. CNTs concentration at about 0.02wt %. There exists an optimal condition for the overall display device performance and maximum system stability that can be obtained by applying proper sonication parameters. Experiment showed that a maximum reduction of 29% in total response time of the nanocomposite can be achieved. In contrast, prolong processing and inappropriate temperature treatments are very likely to bring negative effect on the microstructure of LC nanocomposites.

1. Introduction

Thermotropic liquid crystal (LC) materials are widely used in the electro-optical (EO) display industry since 1971[1]. Over 40 years of technological development in EO display, liquid crystal display (LCD) becomes an essential part of human life and it is beneficial to everyone. For example, LCD is found in many applications such as TV monitor and so on. Among the different phases of LC materials, the nematic one is the most popular type in the LCD industry because of its attractive features such as low power consumption and high contrast ratio. (Power consumption of LCD is 60-300W. For plasma display, it is about 300-660W. The contrast ratio for LCD is 350:1-3000:1. For plasma display, it is about 1000:1 to 4000:1)[2]. The advanced technology reduces the selling price and that is why LCD has dominated the display market with more than 80% unit share[3]. However, LCD has slower response time when it is compared with plasma display panel (PDP) or organic light emitting diode (OLED)[2]. As a result of increasing popularity of fast response application like 3D TVs, the demand for further improvement is aroused. To achieve this, the LC rotational viscosity needs to be reduced and one way to do that is to introduce nanoparticles such as carbon nanotubes (CNTs) into the LC host. Recently, a number of studies on liquid crystal nanocomposites have shown that the operating voltage and switching behavior of LCD can be improved by adding a small amount of CNTs[4-9]. Some studies also proved that the image sticking problem[10] and field screening[11] effect can be suppressed by adding a small amount of CNTs. In terms of switching performance, some of them showed that it was improved due to the reduction of rotational viscosity[4] but the others explained it with increase in rotational viscosity[6,9]. There is a contradiction among the results and it is probably because of the difference in CNTs concentration. It is believed that there exists an optimal CNTs content for the best LCD performance.

Meanwhile, CNTs are perhaps one of the most interesting materials in the research area during the past decade. Because of its extraordinary electronic and mechanical properties[12-14], it has been a promising candidate for high elastic modulus reinforced fibers and polymer composite[15] or nano-scale electronics and transistors[16-19]. To make use of the outstanding properties and for many applications, an uniform alignment of CNTs is essential. Moreover, the ability to give the nanotubes a predetermined direction is also very important. Nevertheless, the current production methods give a random orientation of CNTs and the nanotubes itself tend to bundle together due to the van der Waals interaction between them. This kind of agglomeration makes it hard to be dissolved well in any organic solvent. Consequently, it obstructs the switching effect of the LC and the display performance. So, an efficient dispersion of CNTs in the LC host has become more crucial for the LC-CNTs hybrid system. Improved dispersion by functionalization of CNTs[20,21] or a better compatibility organic solvent[22] was discussed. In contrast, a limited studies related to the optimization of the dispersion parameters were reported.

The aims of this project are to study the effects of: (1) CNTs concentration (0wt% to <1wt%); and (2) dispersion processing parameters (e.g. time, temperature) on the electro-optical performance (e.g. threshold voltage and response time) of LCD. By this, the optimal CNTs concentration and dispersion parameters can be found. Furthermore, we can understand how to achieve the best EO performance by CNTs dopant and how to minimize the agglomeration and obtain efficient & reliable dispersion. This will be achieved by dispersing MWCNTs of a given concentration in LCD using ultrasonic probe at the LC nematic and isotropic temperature range for 30mins. The thresold voltage and response time were determined by a Ne-He laser source and its corresponding detector with computer data logging software. The microstructure and thermal behaviour of LCD doped with CNT were studied using polarised light microscopy and differential scanning calorimetry, respectively.

1.1 Literature review

1.1.1 Introduction to nanocomposite

Composite materials are engineered or naturally occurring materials made from two or more constituent materials with significantly different physical or chemical properties. They remain separate and distinct at the macroscopic or microscopic scale within the finished structure. In terms of nanocomposite, it is a multiphase material where one of the phases has one, two or three dimensions of less than 100 nanometers (nm), or structures having nano-scale repeat distances between the different phases that make up the material[23]. The properties of composite material are highly depends on the ratio of the constituent materials. For example, high stiffness can be achieved by adding larger mass fraction of carbon fiber into carbon-fiber reinforced materials. But when material is in the nano scale, the mechanical, electrical, thermal, optical, electrochemical, catalytic properties will differ markedly from that of the original materials and this situation fully adapt to nanocomposite. The properties of nanocomposites differ from conventional composite materials because of the extraordinarily high surface to volume ratio or aspect ratio. The area of the interface between the matrix and reinforcement phase is typically an order of magnitude greater than the conventional composite materials and the percentage by weight of the nanoparticles introduced can remain very low (on the order of 0.5wt%-5wt%). In general, composite or nanocomposite materials are designed to improve the certain properties of the matrix material by adding a small amount of second phase into the matrix.

1.1.2 History of LC materials

The liquid crystalline nature of cholesterol was first found by an Austrian physiologist called Friedrich Reinitzer by extraction from carrots in 1888[24]. He found that cholesteryl benzoate does not melt in the same manner as other compounds but with two melting points. At 145.5 °C it melts into a cloudy liquid and at 178.5 °C it melts again into a clear liquid. Remarkably, the phenomenon is reversible. By further examination in collaboration with Otto Lehmann & von Zepharovich, the intermediate cloudy fluid was found to be crystalline. By that time, Reinitzer had described three important features of cholesteric liquid crystals: 1) the existence of two melting points, 2) the reflection of circularly polarized light, and 3) the ability to rotate the polarization direction of light.

After Reinitzer's accidental discovery, he did not study liquid crystals further. But it was continued by Lehmann as he realized that he had encountered a new phenomenon. Lehmann started a systematic study, the first material is cholesteryl benzoate, and then of related compounds which exhibited the double-melting phenomenon. He was able to make observations in polarized light. Using his microscope equipped with a hot stage maintained at high temperature. The intermediate cloudy phase clearly sustained flow, but other features under a microscope, convinced Lehmann that he was dealing with a solid[25].

Lehmann's work was significantly expanded by a German chemist called Daniel Vorländer, who had synthesized most of the liquid crystals known from the beginning of the 20th century until his retirement in 1935. However, liquid crystals were not popular among scientists and the material remained a pure scientific curiosity for about 80 years[26].

Later in 1969, Hans Kelker succeeded in synthesizing a substance that had a nematic phase at room temperature, MBBA (Fig.1.1), which is one of the most popular subjects of liquid crystal research[27]. Next, the commercialization of liquid crystal displays was the synthesis of further chemically stable substances (cyanobiphenyls) with low melting temperatures by George Gray[28].

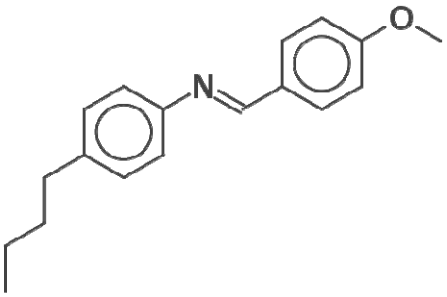

Figure 1.1 Chemical structure of N-(4-Methoxybenzylidene)-4-butylaniline (MBBA) molecule

1.1.3 Liquid crystal structure, phases and properties

Liquid crystal is a state of matter that is intermediate between the crystalline solid and the amorphous liquid. It can be also regarded as a liquid with ordered arrangement of molecular orientation[29] and it has anisotropic mechanical, electric, magnetic and optical properties. A LC molecule has a rod-like structure (Fig.1.2) with rigid core and flexible alkyl chains. It has an aspect ratio from around 3 to around 10 and the rod-like molecular shape is responsible for the anisotropic properties.

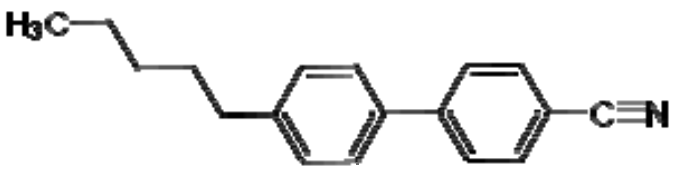

Fig. 1.2 Structure of 4-Cyano-4'-pentylbiphenyl (5CB) molecule

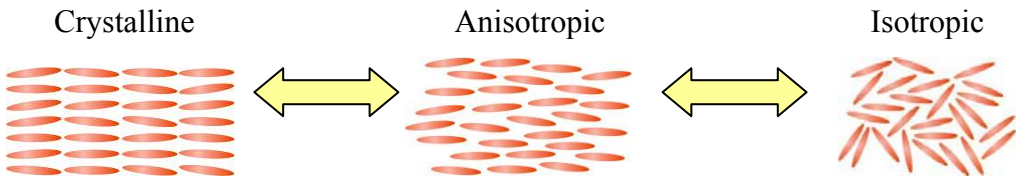

Fig. 1.3 Transformation between different phases

In general, phase transformation between crystalline, anisotropic and isotropic phases is reversible (Fig1.3) and it can be obtained by either dissolving in some solution (lyotropic) or by heating or cooling (thermotropic). There are three phases of liquid crystal: Nematic, smectic, and cholesteric[30]. (Fig. 1.4) Nematic liquid crystals, most widely used phase, have threads distributed all over the area. The molecules should be more or less parallel to each other and it can move in all directions with free rotation along the long molecular axes. The average direction of the long axes of the molecules is called director **n**. Nematics have fluidity similar to that of ordinary (isotropic) liquids but they can be easily aligned by an external magnetic or electric field. Aligned nematics have the optical properties of uniaxial crystals and this makes them extremely useful in displays. Smectic phase have layered structure and the layers can slide over each other and give rise to the flow characteristics. It can be divided into several subclasses by different molecular arrangement inside the layers. In the Smectic A phase, the molecules are oriented along the layer normal, while in the Smectic C phase they are tilted away from the layer normal. These phases are liquid-like within the layers. There are many different smectic phases, all characterized by different types and degrees of positional and orientational order[31]. Cholesteric phase can be viewed as the nematic state superimposed with the natural twist. That means the average direction of the molecules in every layer is unidirectional skewed to the layer just below it.

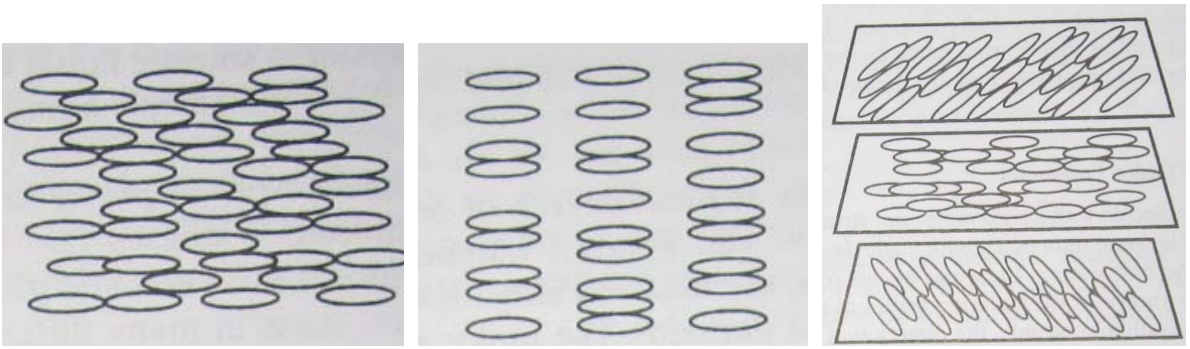

Fig. 1.4 LC phases: Nematic (left), smectic (middle), and cholesteric (right)

For thermotropic LCs such as 5CB, it has a nematic temperature range from around 24°C to around 35°C [32]. At room temperature, it is in nematic state and it is a cloudy liquid. But when it was heated up to 35°C, the nematic-isotropic transition occurs and the liquid turns into a clear one. This temperature is also known as clearing temperature/ point.

Orientational order parameters, elastic constant, rotational viscosity and dielectric anisotropy are the most important physical properties of LC material because the EO characteristics of LCD such as driving voltage, contrast ratio and response time are strongly depend on these properties[30].

An order parameter is a measure of the degree of order in a system[33]. For rod-like molecules, the direction of the long axis is often chosen as the unit vector representing the orientation of the molecule. But in fact the molecule structure may not be symmetric with respect to a rotation around the long axis. In the nematic phase of most liquid crystals, the long axis is aligned approximately parallel to one another. This leads to a longitudinal orientational order and the transverse orientation of the molecules remains random. The longitudinal order parameter S of liquid crystal is defined as

$$S = \frac{1}{2}(3\cos^2\theta - 1)$$

where θ is the angle between the long axis of an individual molecule and the director **n**. For perfect parallel alignment, $\theta = 0^{\circ}$ and S = 1, while for totally random orientation, S = 0. The value of S depends on the structure of the molecule, normally in the range between 0.4 to 0.6. However, it is strongly temperature dependent. At the clearing point, S = 0.

Like most liquids and solids, liquid crystals exhibit curvature elasticity. The elastic constants of a liquid crystal determine the restoring torques that arises when the system is perturbed from its equilibrium configuration. In LCD, electric field is often applied to cause a reorientation of the molecules. The static deformation of LC is determined by the balance between the electric torque and the elastic restoring torque and it can be divided into a combination of three basic deformations: splay, twist and bend. For an isothermal deformation in an incompressible fluid, the free energy/ elastic energy can be written as a quadratic function of the curvature strain tensor. Followed by Oseen-Frank theory[34,35], the elastic energy density of a deformed LC can be expressed as

$$F = \frac{1}{2}k_1(\nabla \bullet n)^2 + \frac{1}{2}k_2(n \bullet \nabla \times n)^2 + \frac{1}{2}k_3(n \times \nabla \times n)^2$$

where k_1, k_2, k_3 are the splay, twist and bend elastic constants respectively. The elastic constants are also strongly temperature dependent and for most LC compounds, the elastic constants are in the range from 3 to 25pN (10^{-12}N).

The viscosity of fluid is an internal resistance to flow and it is defined as the ratio of shearing stress to the rate of shear. It arises from the intermolecular forces in the fluid and it has a profound effect on the dynamical behavior of LCDs. At low temperature, the viscosity increases due to the lower molecular kinetic energy and this can severely limit the switching of LCDs. Whereas, viscosity decreases at high temperature. For most nematic LC used in displays, the value of viscosity is ranged between 0.02 to 0.5 Pa·s. As a comparison, water at

25℃ has a viscosity of around 0.89 mPa·s[36]. By experiment, it is known that molecules with a higher number of rings or longer alkyl chains exhibit higher viscosities. In addition, due to the stronger polar interaction between molecules, higher viscosities usually show on LC with high value of dielectric anisotropy.

Due to the uniaxial symmetry of the rod-like LC molecules, the dielectric constants differ in value along the preferred axis ($\varepsilon_{\parallel}$) and perpendicular axis ($\varepsilon_{\perp}$). The dielectric anisotropy is defined as

$$\Delta\varepsilon = \varepsilon_{\parallel} - \varepsilon_{\perp}$$

The sign and the magnitude of the dielectric anisotropy are the most important feature of LC material in LCDs. For liquid crystal with positive dielectric anisotropy ($\varepsilon_{\perp}<\varepsilon_{\parallel}$), the lowest electrostatic energy occurs when the director is parallel to the applied field. For typical rod-like LC molecule, the dielectric anisotropy is always positive because the longitudinal polarizability is usually greater than the transverse polarizability. However, for polar LC compounds, the dipole contribution can cause an increase or decrease of $\Delta\varepsilon$ and eventually lead to a negative $\Delta\varepsilon$ like MBBA. (Fig. 1.1) Dielectric anisotropy is again temperature dependent and it approaches to zero at the clearing point. In addition, it depends on frequency of the applied electric field. Some LC mixture exhibits a positive dielectric anisotropy at certain frequency, and a negative dielectric anisotropy when the frequency increases or decreases. This kind of material with such a reversal of dielectric anisotropy is known as dual-frequency material.

1.1.4 Application of LC material

Nematic LC materials are widely use in display devices. This kind of devices have their

attractive features such as flatness, low power consumption, high contrast ratio and full-color capability[1]. LC materials can apply to all common display devices from wrist watches, clocks to highly sophisticated thin-film-transistor (TFT) laptop or TV monitors. Each application has different features to fit the special needs and those LCD characteristic are listed in table 1.

Type of application	Image of display	Operation temperature	Typical response time
STN character LCD (Home appliance)		-20 to +70°C	280ms
STN character LCD (Medical use)		-30 to +80°C	115ms
STN Graphic LCD (Handheld products)	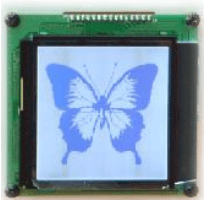	-20 to +70°C	400ms
STN Graphic LCD (Industrial products)		-20 to +70°C	345ms
Color TFT (Handheld products)		-20 to +70°C	40ms
Color TFT (Automotive)		-30 to +85°C	20ms
All the above data are from Microtips Technology, Inc.[37]			
TFT LCD TV		0 to +40°C	8ms
3D TFT LCD TV		0 to +40°C	6ms
All the above data are from Sharp Electronic Ltd. [38]			

Table 1 LCD characteristics for various applications

In the display industry, the liquid crystal materials are always used as a mixture of different series of LC rather than an individual one. This is mainly due to the requirements of the real applications. Some of them may need to be operated at extreme temperature with reasonable response time and various LC mixing formula were prepared by different manufacturer to compromise all features related to applications. It is also important that thermotropic LCDs operate at the temperature of the nematic range only. For 5CB, the nematic temperature ranges from around 24°C to 35°C[32]. That means the LCDs with 5CB can only function with this range. Out of this range, abnormal display or no display can be observed. In addition AC voltage is applied to LCDs. This is because DC causes the ion-charge effect and gives rise to flickering and image sticking problems.

Other than LCDs, nematic phase is also used for other electro-optic devices such as electrically controlled wavelength filters and optical switches.

1.1.5 History of Liquid Crystal Display (LCD)

The first LCD was made when George Heilmeier and his colleagues discovered four new electro-optic effects in liquid crystals in the 1960s[39,40]. It was called the dynamic scattering mode (DSM). However, it was not commercialized due to its poor quality. Later on in 1971, when the first Twisted Nematic (TN) display was produced, replaced the DSM display and started to dominate the industry because of its attractive features such as lower operation voltage and power consumption[41]. Within forty years of development, many different modes for nematic LC displays were suggested and invented, such as the super-TN (STN) mode[42], the optically compensated bend (OCB) mode[43], the in-plane switching (IPS) mode[44], the vertical alignment (VA) cell mode[45], and the hybrid TN (HTN) mode[46]. Nowadays, LCDs are definitely the mainstream of the display industry and almost everyone around the world relies

on it in their daily life. In recent years, the increase number of 3D television application has driven the important of LCDs with faster switching time.

1.2 Structure and working principle of LCD

1.2.1 Basic structure of LCD

A standard LCD consists of several different layers. To make it simple, it is liquid crystal material sandwiched between two Indium tin oxide (ITO) glass substrates with one polarizer attached on each of the glass substrate. (Fig. 1.5) The pattern (character or graphic) of the ITO layer can be made by a series of processes like resist coating, UV exposure, developing and etching. These processes are based on the photolithography[47] technique and the patterns of these electrodes will determine the shapes that will appear when the LCD is turned on. Typically, the two polarizers are in crossed configuration, i.e. one is filtering the vertical light and the other is filtering the horizontal one. The reflective film at the back may not necessarily be attached. It depends on the display mode and in some occasions, a backlight source will be replaced. The overall thickness of the LCD is mainly determined by the thickness of the glass substrate as the polarizers are relatively thin. Typically, the thickness of LCD is smaller than 1cm. And the distance between two glass electrodes (cell gap) is around 5-30 micrometers.

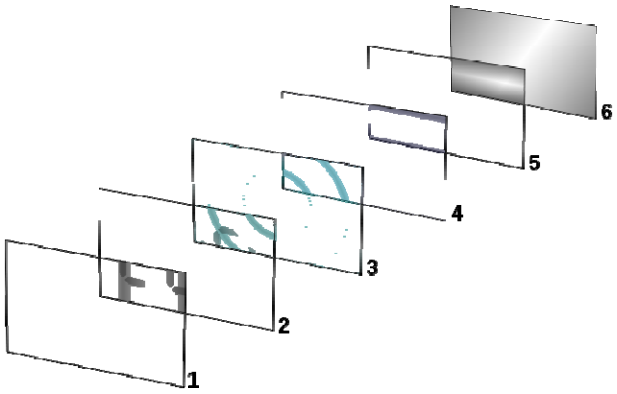

Figure 1.5 Basic structure of LCD. No.1&5: Polarizer film. No.2&4: ITO glass substrate.

No.3: Liquid crystal layer. No.6: Reflective film (Optional)

1.2.2 Materials

1.2.2.1 Substrate & electrode

Glasses are commonly used as substrates. It is an excellent material for substrates because it has a flat surface and highly transparent. It has high corrosion resistance for chemical as well. Also, glasses have very low moisture permittivity. This can slow down the diffusion of moisture and oxygen to the liquid crystal layer. However, glasses are not flexible and brittle and plastic substrates may be another choice. It is light weight, flexible and not easy to break. But plastic substrates have poor thermal resistance and moisture can pass through it easily.

ITO is commonly used as electrode of LCD and it is coated on the glass substrate by sputtering [48]. It is smooth, conductive and transparent. Also, ITO can be etched easily to make the display pattern and it is thermal stable to go through some processes in high temperature during manufacturing. The thickness of the ITO layer is about several hundreds nanometers and it controls the surface resistivity. For example, the surface electrical resistance decreases with increasing ITO thickness.

1.2.2.2 Polarizer

Other than the ITO glass and LC, polarizer is the most important material in LCD. A polarizer is a device that converts a beam of electromagnetic (EM) waves/light of undefined or mixed polarization into a beam with well-defined polarization. There are different types of polarizers. Absorptive polarizer is made of plastic material such as polyvinyl alcohol (PVA) plastic with an iodine doping and those molecules are aligned in one particular direction. Electrons from the iodine dopant are able to travel along the chains, ensuring that light polarized parallel to the chains is absorbed by the sheet; light polarized perpendicularly to the chains is transmitted (Fig. 1.6). If two polarizers are placed in crossed configuration (perpendicular to each other), almost all the light was blocked and a dark area can be observed.

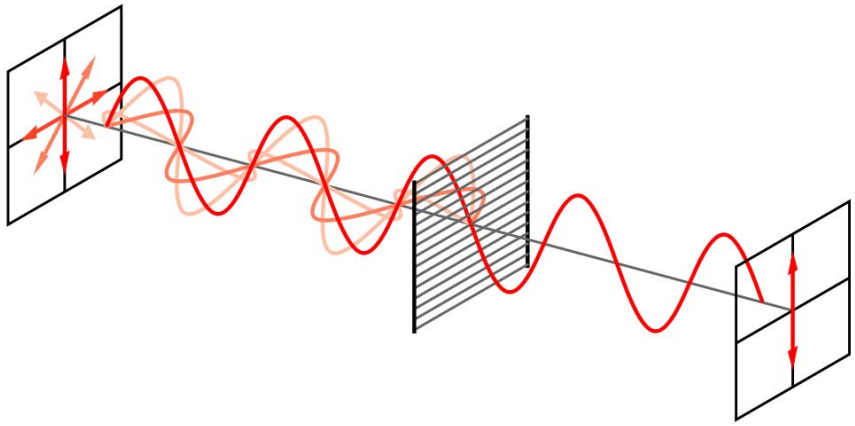

Figure 1.6 A bidirectional light source pass through a polarizer and become unidirectional

When light reflects at an angle from an interface between two transparent materials, the reflectivity is different for light polarized in the plane of incidence and light polarized perpendicular to it. Light polarized in the plane is said to be p-polarized, while that polarized perpendicular to it is s-polarized. Reflective polarizer is made of a stack of tilted plates at Brewster's angle (No p-polarized light is reflected from the surface) to the beam. For visible light in air and typical glass, Brewster's angle is about 57°, and about 16% of the s-polarized

light present in the beam is reflected for each air-to-glass or glass-to-air transition. It takes many plates (More than 10 plates) to achieve even mediocre polarization of the transmitted beam with this approach and it is not very useful. A more useful polarized beam can be obtained by tilting the pile of plates at a steeper angle greater than Brewster's angle yields a higher degree of polarization of the transmitted beam. For angles of incidence steeper than 80° the polarization of the transmitted beam can approach 100% with as few as four plates, although the transmitted intensity is very low in this case. Adding more plates and reducing the angle allows a better compromise between transmission and polarization to be achieved.

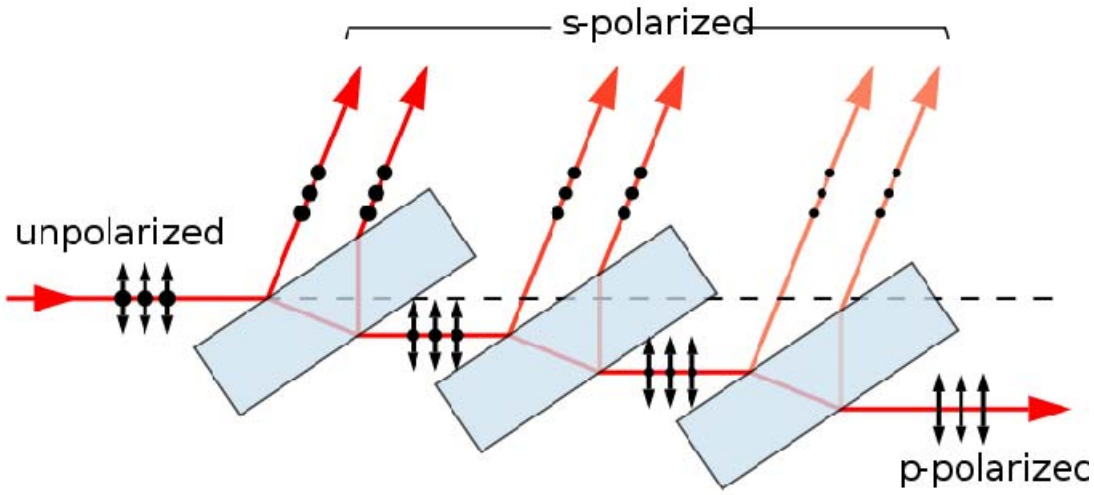

Figure 1.7 A stack of plates at Brewster's angle to achieve polarized light. Full polarization requires many more plates than shown.

1.2.2.3 Alignment layer

Alignment layer is generally plastic thin film which made of polymer material such as polyimide and it is located on the top of the ITO layer on both glass substrates. It aims to generate groove to align the liquid crystal molecules in a particular direction and this direction is controlled by unidirectionally mechanical rubbing on the thin layer with a cloth or similar material. The rubbing angle between two glass substrates and the polarizer configuration vary

from different display modes. For normally white (NW) mode or positive mode, the rubbing angle of the two glass substrates is perpendicular to each other and crossed polarizer configuration is applied. For normally black (NB) mode or negative mode, the rubbing angle of the two glass substrates is parallel to each other and parallel polarizer configuration is applied. (Fig. 1.7)

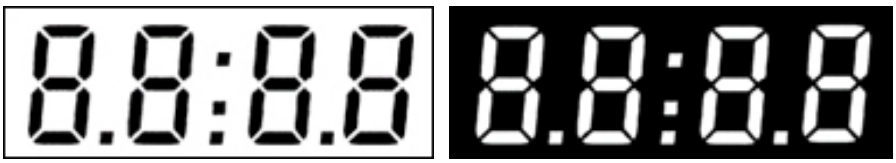

Figure 1.8 Positive mode (left) & negative mode (right)

1.2.2.4 Insulating layer & spacer

Although the two ITO electrodes are facing inwards to each other with around 5-30μm distance apart, they are actually not contacting with each other and no electricity should pass through it. Otherwise, the display will not work at all. In the industry, a polymer base insulating layer will be coated on the alignment layer to avoid short circuit between electrodes.

Even though the cell gap is so small, it is important to maintain it at a uniform distance. Otherwise, the background color of the LCD will be uneven and caused optical defects such as discoloration. This problem is more common in a large display because of the larger cell gap area. In the industry, very small glass or plastic balls are used as spacer and they will be sprayed on the substrate to maintain a uniform cell gap.

1.2.2.5 Carbon nanotubes (CNTs)

Functionalized multi-walled carbon nanotubes (MWCNTs) with carboxyl groups are the nanoparticle chosen to be dispersed into LC and they are highly anisotropic as well. In terms of morphology, carbon nanotubes are categorized as single walled (SW) with a sheet of graphite rolled into a cylindrical nanostructure and multi walled (MW) are with multiple rolled layers (Fig. 1.8). They are usually produced by arc-discharge[49], laser ablation[50] or chemical vapor deposition[51] (CVD). No matter how many layers they are, they have extreme large length-to-diameter / aspect ratio (up to 132,000,000:1)[52] and other extraordinary characteristics like excellent mechanical and electrical properties. Carbon nanotubes (CNTs) are the strongest and stiffest materials yet discovered in terms of tensile strength and elastic modulus respectively and it can achieved tensile strength as high as of 60-100GPa[53,54]. In the electrical point of view, CNTs has electric current density of 4×10^9 A/cm^2, which is more than 1,000 times greater than metals such as copper[55]. Because of all of these outstanding features, CNTs are the promising candidate for novel electric devices such as electron field emitters[56,57], sensitive gas detectors[58,59] and nanoscale rotational actuators and motors[60].

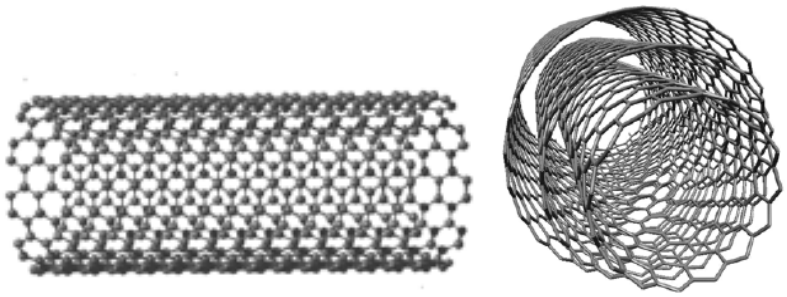

Figure 1.9 Single-walled carbon nanotube (left) & multi-walled carbon nanotube (right)

However, CNTs are difficult to handle because strong van der Waals forces cause bundling and the formation of aggregates. So, good and stable dispersions formed by isolated CNTs can hardly be obtained. If the CNTs are not uniformly distributed, the exceptional properties

can not be shown and that is why effective dispersion is critical for the whole LC nanocomposite hybrid system.

1.2.3 Working principle of LCD

Under the crossed polarization condition and without electric field, the display should be dark. Nevertheless, the twisting nature of LC cancels the crossed polarization and the display shown a background color which depends on the type of polarizer that are using.

When an electric field is applied on LC molecules, the director can be reoriented and this is known as the Fréedericksz transition[61,62]. It is a transition in liquid crystals produced when a sufficiently strong electric or magnetic field is applied to a liquid crystal in an undistorted state. Below a certain field threshold voltage the director remains undistorted, but as the electric field value is gradually increased from this threshold, the director begins to twist until it aligned with the field. (Fig. 1.9) At this moment, the twisting characteristic of LC disappeared and crossed polarization shown. This is why the etched ITO pattern turns dark when an appropriate electric field is applied.

In LCDs, the voltage supplied converts into an optical polarization behavior as the Fréedericksz transition leads to a change in the birefringence property of the cell, and thus a change in transmission of it. The switching (ON-OFF) effect of LCD can be shown by changing the voltage around the threshold.

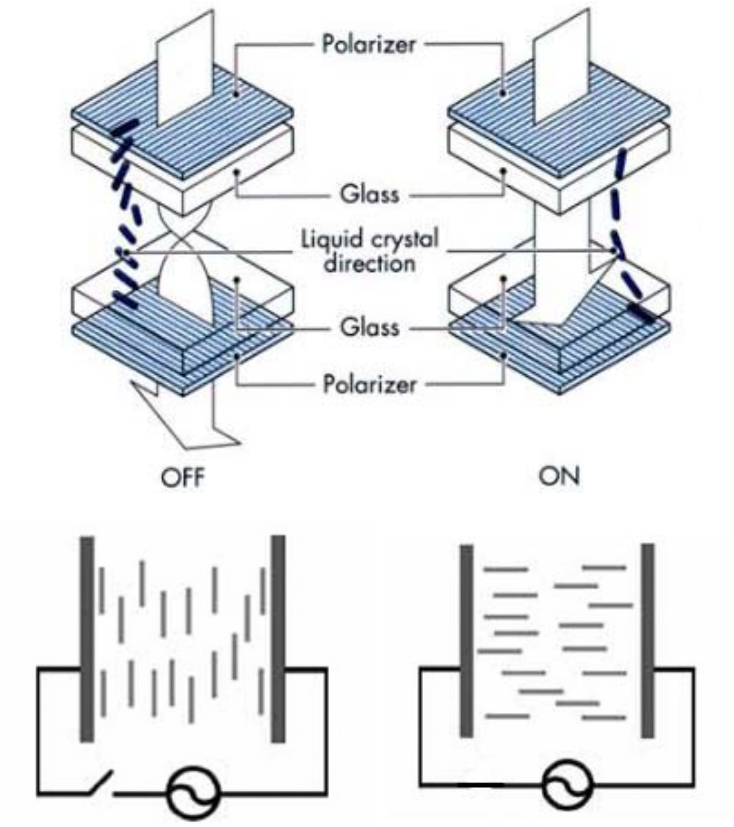

Fig.1.10 Director change in LC molecules when the applied voltage is off (left) & on (right)

1.3 Definition of LCD characteristics

Fig. 1.10 is a typical of brightness and operating voltage relationship for normally white (NW) mode LCDs. When the applied voltage is low, the LC molecules remain at the original position and the display still white. (i.e. brightness is 100%) When the voltage gradually increases, the LC molecules start to re-orientate until they are parallel to the electrical field. The brightness begins to drop until it reaches a certain level of brightness. (i.e. brightness is 0%) After that, the display will keep in the same contrast even after the voltage is extended.

For normally black mode LCDs, the brightness/ voltage relationship is completely reversed. (0% brightness shown with no voltage applied and 100% brightness shown with voltage above threshold.)

The threshold voltage (V_{th}) and the driving voltage (V_{on}) are defined as the voltage where the transmitted light intensity is decreased to 90% and to 10% of the initial value at null voltage respectively (Fig. 1.10). From equation, V_{th} can also define as follow:

$$V_{\text{th}} = \pi \sqrt{\frac{k_{ii}}{\epsilon_0 |\Delta\epsilon|}} \qquad \text{(Equation 1.1)}$$

where k_{ii} (i = 1,2,3) are the splay, twist and bend elastic constants respectively, ε_0 is the permittivity of free space and $\Delta\varepsilon$ is the dielectric anisotropy.

The ratio of driving voltage and threshold voltage (Von/ Vth) is known as steepness. It is a good indicator to evaluate the LCD performance. The smaller the steepness, the better the contrast ratio and viewing angle are.

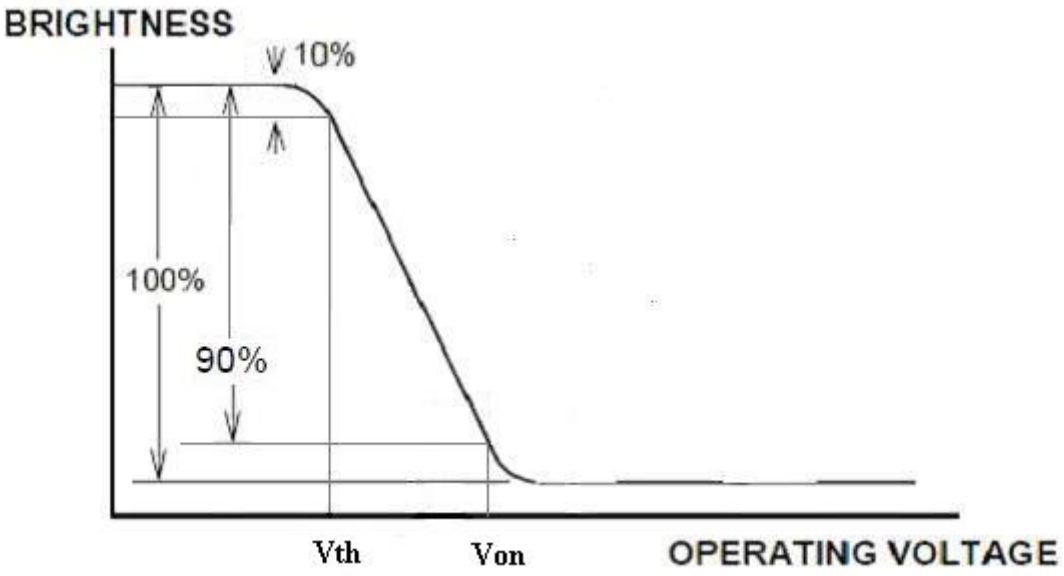

Fig. 1.11 Relationship between brightness and operating voltage of NW mode LCD

The definition of LCD response time is illustrated in Fig. 1.11. During a normal switching, the LCD will turn from white to black and white again or vice versa. At the same time, the brightness will change correspondingly with a rising and a falling brightness. The response

time is the sum of the rise and fall time, where rise time (τ_{on}) is the time for the brightness change from 10% to 90% and fall time (τ_{off}) is the time for the brightness change from 90% to 10% under a 1 kHz pulse voltage excitation. In ideal case, the two should be more and less the same. By equation, the rise time and fall time can be expressed as follow:

$$\tau_{on} = \frac{\gamma_1 d^2}{\epsilon_0 |\Delta\epsilon| V^2 - k_{ii}\pi^2} \quad \text{(Equation 1.2)}$$

$$\tau_{off} = \frac{\gamma_1 d^2}{k_{ii}\pi^2} \quad \text{(Equation 1.3)}$$

where k_{ii} (i = 1,2,3) are the splay, twist and bend elastic constants respectively, ε_0 is the permittivity of free space, $\Delta\varepsilon$ is the dielectric anisotropy, d is the cell gap and γ_1 is the viscosity.

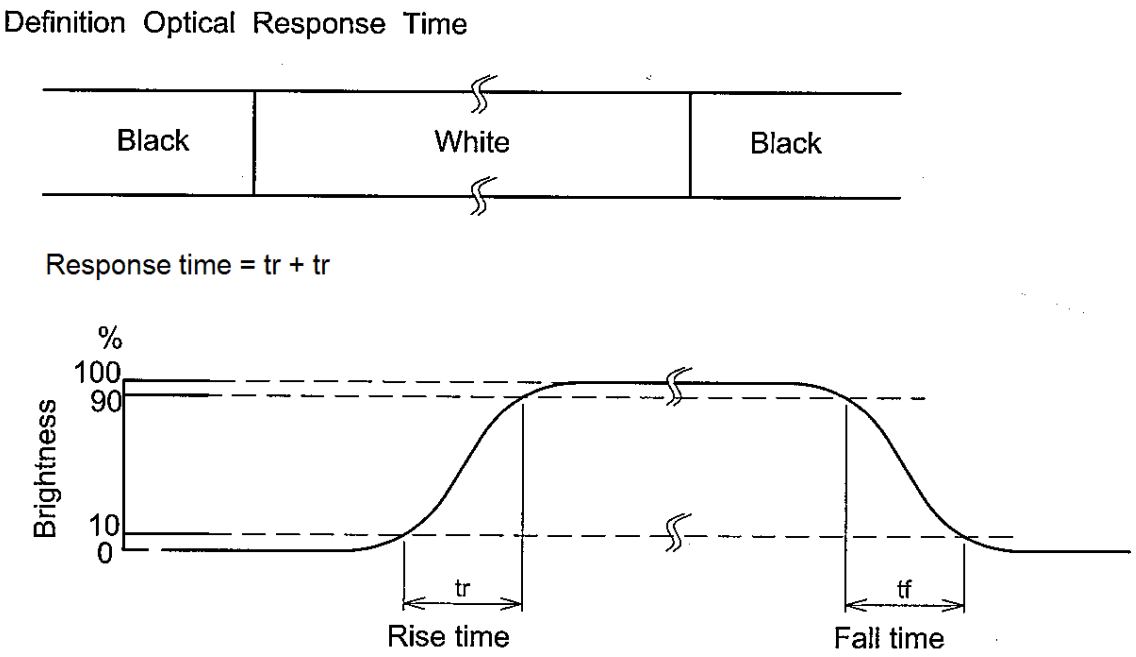

Fig. 1.12 LCD response time definition

1.4 Other LC nanocomposites material

Other than nematic LC and CNTs, many LC nanocomposites have been studied. Nanoscle ZnO can be doped into the ferroelectric liquid crystal. It showed an increment of contrast ratio of the cell and enhancement in electro-optical response by increasing the dynamic polarization[63]. Experiments also suggested that ferroelectric nanoparticles such as $Sn_2P_2S_6$ or $BaTiO_3$ can increase the order parameter of nematic LCs[64]. Lower operating voltage and better switching behavior were observed in different LCD switching modes such as VA (vertical alignment). They include the doping of nanoscale inorganic particles like Pd, MgO or SiO_2. 5CB doped with the metal nanoparticles Ag-Pd composite exhibited a frequency modulation (FM) EO response with short response time of milliseconds (ms)[65,66]. Inorganic nanoparticles like MgO or SiO_2 also showed positive impact on nematic LC material. Studies reported that reduction of threshold voltage ad decrease in order parameter can be achieved by doping MgO[67] or SiO_2[68].

Semiconductor nanowires like CdS were doped into LC media too. By combining the new nanostructure material with the currently mature LCD technology, a new approach to manipulate the polarization of the emission from semiconductor nanorods by an external bias was reported[69].

1.5 Methods to align CNTs

As mentioned above, the alignment of CNTs is important because CNTs are highly anisotropic and those superb properties can only be revealed with proper alignment. One approach is based on aligning the nanotubes during their growth in the direction perpendicular to the substrate[70,71] or parallel to the substrate[72]. This method allows the growth of tube in

selected areas and with a certain control of the tube length. But there are limitations on the density of CNTs and the control of the presence of impurities. Another approach is the post-growth techniques with electric[73,74] or magnetic field[75,76]. This method aligns the CNTs along the field direction in different fluid media but the alignment will be disappeared with the absence of the external field. In general, no method can be regarded as satisfactory, providing large scale and good quality alignment of CNTs, easily and independently of the type of CNTs employed.

This is where LC materials enter the picture. With the self-organization nature of LC, it is an alternative way of align CNTs with dispersion. The CNTs in LC can be well aligned with the director of the LC molecules and it can be done by dispersed a small amount of CNTs into LC by ultra-sonication. Other than the alignment, what makes LC attractive is that its direction follows the change of the external electrical or magnetic field. When CNTs is dispersed, it manipulates its orientation as well and make it possible to apply in some novel application like nano-switches[77,78]. Moreover, the LCD switching technology is a mature technology to be mass produced in the industry.

1.6 Dispersion methods

There are mainly three different methods. The first one is to disperse nanotubes in organic solvents in low concentrations followed by a mixing with a LC medium[79,80]. The mixture is properly sonicated to prevent the aggregation of the CNTs inside the solution. The dispersant counteracts the van der Waals attraction of adjacent CNTs by introducing sufficiently strong repulsive force between them. After evaporating the solvent, the LC/ CNTs suspension becomes ready for use. However, one of the drawbacks of this dispersion technique is the undesired solvent effect and some specific solvent can even form LC phases with proper modification of the CNTs surface by oxidation[81].

The second method is adding a small amount of CNTs (not higher than ~ 0.1 wt%) into the LC material directly followed by proper percolation and sonication[4]. It has been realized that the second procedure involving no solvents is much more reliable than the former approach. However, it has been noticed from the investigations involving SEM that a part of the dispersed CNTs aggregates in bundles before ultrasonic treatment.

The third method employs surface modification of CNTs for enhanced compatibility[82]. Such surface modification is usually carried out by surfactant encapsulation or chemically covalent functionalization through reactions onto the p-conjugated skeleton of CNTs[83]. Although chemical functionalization was proposed to be a promising means to promote the dispersability of CNTs in organic solvents, it should be noted that covalent surface functionalization can affect intrinsic mechanical, electrical and optical properties of nanotubes as well[84].

1.7 EO performance of other LC-CNTs hybrid system

As mentioned above, there are lots of studies showing an enhancement of the EO performance of the display with CNTs doped LC material. Chen et al. studied E7/ CNTs with 0.01-0.1 wt% and faster response was recorded with dilute suspensions (0.01-0.05 wt%) due to the decrease in rotational viscosity[4]. Lee et al. also showed almost 50% decrease in the threshold voltage with 5CB and 0.02 wt% MWCNTs. This is attributed to the large dielectric anisotropy of the high aspect ratio CNTs and to the parallel orientation of the CNTs to the LC director[5]. Huang et al. worked on E7/MWNTs and showed a significant improve in threshold voltage. There is a 12.6% decrease when the CNTs concentration is 0.01 wt%. However, the response time increases from 88ms to 270ms when the CNTs concentration increases from 0 to 0.01wt%[6]. On the other hand, Huang et al. worked on vertical alignment (VA) LC. A

step-voltage driving scheme is demonstrated to eliminate the optical bounce and effectively improve the rise time of the cell. Under the CNT doping condition and the step-voltage driving scheme, the response time of the VA LC cell can be reduced to 50% of that of the pristine cell under the conventional driving scheme[85]. Consistent results can not be seen among different studies. The EO performance of the LCD is quite dissimilar with a wide variety of CNTs and LC material combinations.

1.8 Summary

There is no doubt that LCD is a relatively mature technology and there is a trend that fast response display will be the mainstream in the future. It is therefore understood that the LCD industries always thirst for LC material with lower rotational viscosity and shorter response time. By doping CNTs into LC media, this target can be achieved and the homogeneous alignment can also be obtained. It is a "win-win" situation for both parties, the CNTs taking advantages of the LC anisotropic or the LC benefiting from the presence of the CNTs. However, the biggest problem with CNTs is they tend to bundle together due to the van der Waals interaction between them. This kind of agglomeration makes it hard to be well dispersed in LC and they are in general insoluble in most of the common organic solvents as well. Also, the agglomeration of CNTs obstructs the switching effect of the LC and the display performance. So, an efficient dispersion method needs to be found out before moving on to further applications. Although CNTs helps to improve the response time for LCD, the amount of dispersion has not been optimized. Many studies proved that the switching effect will be disturbed by the excess amount of CNTs. So, there should be a critical dispersion quantity of CNTs to optimize the LCD performance.

Another important issue is the stability after dispersion. Even the mechanical action during sonication is sufficient to get an immediate distribution of CNTs to form a macroscopically black suspension. The stability of dispersion of CNT in LC medium with time is not yet known. This is really important because good stability and durability are crucial elements before it brings to the competitive market. So, the optimal CNTs concentration in the LC nanocomposite system and the effect of the dispersion parameters will be found out in the following sections.

2. Experimental methods

The experimental methods of the whole study were divided into four parts and they are LC/ MWCNTs dispersion, LCD cell preparation, material characterization and electro-optical behavior measurement.

2.1 LC/ MWCNTs dispersion

In order to achieve a good dispersion of CNTs in LCD, 1,2-Dichloroethane (DCE) from Sigma-Aldrich Co. was used as a surfactant. The COOH functionalized MWCNTs used in the experiment have outer diameters of 8-15nm and length of 10-50μm. It was synthesized by catalytic chemical vapor deposition (CCVD) and it was supplied by Cheap Tubes Inc. (USA). It has a COOH content of 2.56wt% and purity of > 95 wt% respectively. It is expected that the functional COOH group induced on the surface of CNTs can help to reduce bundle formation and enhance the dispersion state[86, 87]. A small amount of MWCNTs powders were dispersed in DCE by sonication for 1 hour under 20 kHz vibration with power of 600 Watts (VXC600, Fig. 2.1). Then, centrifuging with 15000 RPM for 30mins (Beckman J2-21 centrifuge, Fig. 2.2) was done and the supernatant (Fig 2.3) was poured out to mix with LC material (4′-Pentyl-4-biphenylcarbonitrile, also known as 5CB. The LC was purchased from Sigma-Aldrich (UK). It has a dielectric anisotropy $\triangle\varepsilon = 11.7$, a range of nematic mesophase from 22.5 to 35.5°C and viscosity of 29.9 mPa.s at room temperature). The mixing of CNTs/DCE to LC was achieved by further sonication for 30 minutes. After that, DCE was removed by solvent evaporator and dispersion of CNT in LC was obtained (Fig. 2.4). CNTs/LC nanocomposites with CNT concentration from 0.01wt% to 1wt% were prepared by the method described as above for this study.

The temperature for ultrasonication during dispersion of CNT in LC was varied from room temperature to below 25ºC. The sub-room temperature was chosen to keep LC in nematic state (e.g. from 24ºC to around 35ºC) and was achieved using ice water bath.

Fig. 2.1 Sonciation under 20kHz

Fig. 2.2 Beckman J2-21 centrifuge

Fig 2.3 Supernatant after centrifuging

Fig. 2.4 LC nanocomposite after dispersion

To study the sonication time effect on LCD performance, another batch of samples were prepared. 1mg of MWCNTs powders were dispersed in DCE with sonication time of 5, 15 & 30 minutes under 20 kHz vibration with power of 600 Watts respectively. Then, centrifuging with 4000 RPM for 30mins (Jouan C422 centrifuge) was done and the supernatant (Fig 2.3) was poured out to mix with 5CB for further sonication for 30 minutes. After that, DCE was removed by solvent evaporator and dispersion was achieved. Various degree of stirring of CNTs/DCE mixture prior to ultrasonication was used. This was achieved by 24 hours stirring of sample with a magnetic stirrer prior to CNTs/DCE dispersion.

2.2 LCD cell preparation

The ITO glasses used in the study are supplied by Sigma-Aldrich Co. with dimension of 25 mm × 25 mm × 1.1 mm (L × W × D) and surface resistivity of 8-12 Ω/sq. The alignment layer used in the LCD cell is polyvinyl alcohol (PVA) from Sigma-Aldrich Co. It has a molecular weight range from 146,000-186,000 and it was 98-99% hydrolyzed. It was prepared to solution by dissolving 0.4g of PVA into 10ml distilled water. The ITO coated glass substrate was dipped into the PVA solution and then lifted out of the solution to dry at room temperature to produce a thin PVA layer. A cleaned ITO glass substrate with PVA coating (Fig. 2.5) was rubbed with cloth in one direction only to promote planar LC alignment along the rubbing direction. The cell was constructed by using two identical substrates with ITO coating side facing each other and the difference in rubbing direction of the two substrates is 90° (Fig. 2.6). After that, the LC/ MWCNTs prepared mixtures were introduced to the sandwich cell by capillary action at room temperature. The cell gap is about 10μm and it was confirmed by the thickness of the PET film on each ITO glass. Finally, a cross-polarizers configuration (From Edmund Optics Ltd with dimension of 8.5 in × 5 in × 0.3 in (L × W × D) and 0.04% transmission under crossed configuration) was carried out on

the non conductive side of the two ITO glass substrates (Fig. 2.7).

Fig 2.5 ITO glass coated with PVA

Fig. 2.6 An assembled LCD cell

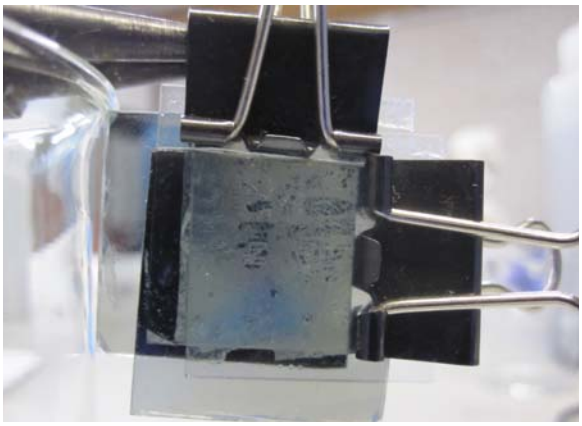

Fig. 2.7 A completed LCD cell with crossed polarizer configuration

2.3 Material characterization

For phase transformation information, DSC (DSC7, Perkin Elmer) calorimetry experiments were conducted on 5CB and LC/ CNTs nanocomposites with temperature range of -20°C to 50°C, in the heating and cooling modes at 5ºC /min. Also, observation with microscope under hot stage (THMS 600) was done to see the microscopic change during phase transformation from 34-36ºC. For CNTs bonding identification, Raman spectroscopy (Renishaw inVia) was performed. For the surface morphology of CNTs, Scanning Electron Microscopy (SEM, Philips XL-30) examination was conducted with 15keV accelerating voltage and secondary electron imaging mode. For angular distribution/ movement of the MWCNTs within the LC

host with respect to the LC director under an applied electric field, polarized optical microscope (Leitz DMRX, 50x magnifications) with transmitted light was used and examination was done with crossed polarizer configuration.

2.4 Electro-optical behavior measurement

For response time of LCD, a He–Ne laser (633 nm, JDSU 1108P) was used as a source in order to characterize the optical transmissions of the samples. The transmission, rise time and fall time of the sample were detected by a photodiode (S120C) and analyzed by a power meter (PM120D) from Thorlabs. The LCD cell (Fig. 2.8) was driven by a function generator (Thurlby Thandar TG210) with square wave and the frequency of the applied voltage was 1 kHz. The applied voltage is from 0V to around 10.5V and the data was logged to the computer. The whole measurement setup is illustrated in Fig. 2.9 below. The center point of the laser source, LCD cell & photodiode should be aligned so that the most appropriate data can be recorded.

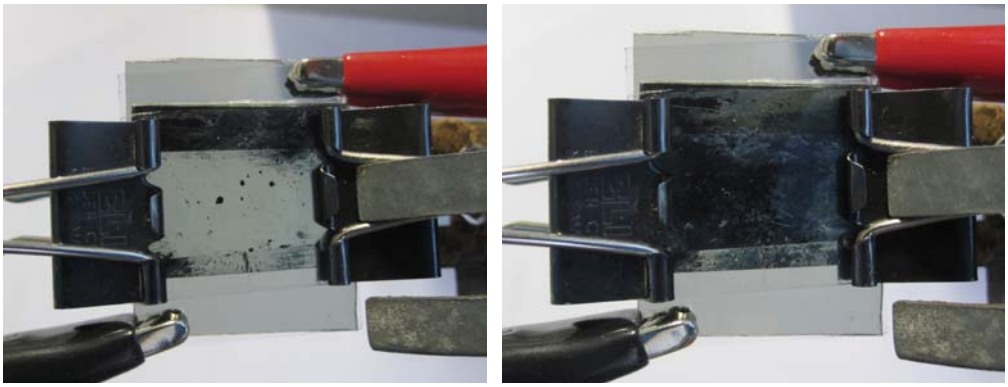

Fig. 2.8 The LCD cell is switched off (left) & on (right)

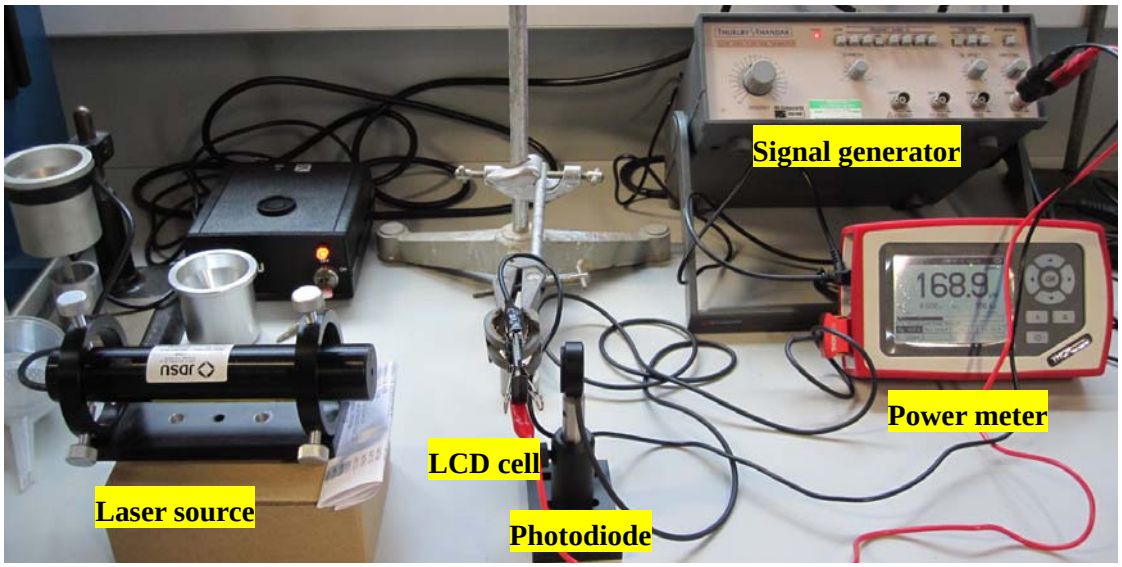

Fig. 2.9 Experimental setup of response time measurement using the intensity of transmitted light

3. Results

3.1 Material characterization

3.1.1 LC material

Fig 3.1 shows the DSC spectrum of 5CB as supplied, obtained with a scanning rate of 5℃/ min. It showed two endothermic and exothermic peaks that correspond to the solid-to-nematic (S-N) and nematic-to-isotropic (N-I) transition of the LC material during heating and cooling cycles respectively. The phase transition temperature (T_{SN} and T_{NI}) during heating of the LC materials are 25.02℃ and 35.26℃ respectively. During cooling, the T_{NI} is 34.07℃ and the T_{SN} is -11.27℃. The solid-to-nematic peaks showed a larger area when it was compared with the nematic-to-isotropic one. It implies that more energy was absorbed or released during the transitions. During the S-N phase change, LC transforms from crystalline to liquid structure, which is similar to the transition from solid to liquid of a material. It involves a large atomic/molecular movement or rearrangement and it needs quite a large amount of energy. Whereas, during the N-I phase change, it changes from an ordered form to a disorder form and a relatively small amount of energy is needed. That is why the S-N phase change show a larger peak area as the energy involved is larger.

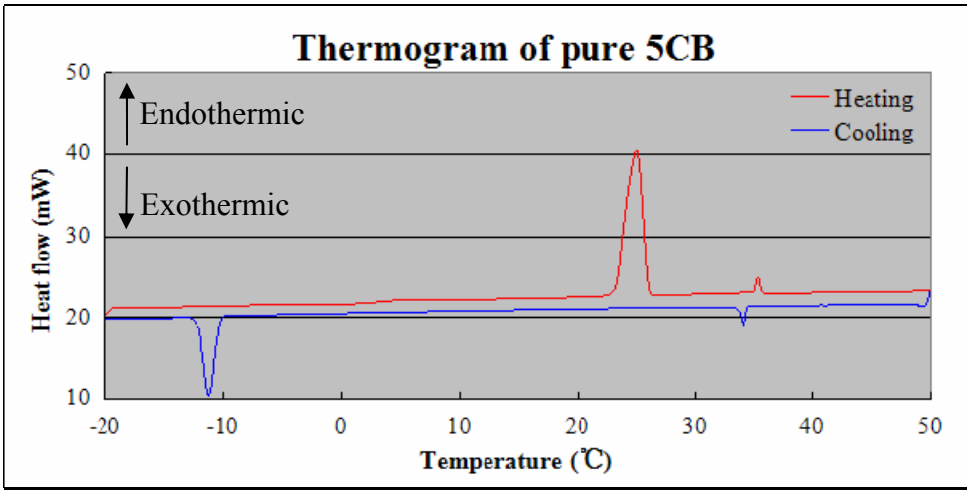

Fig. 3.1 Thermogram of pure 5CB during heating and cooling

In addition, the results suggested that both S-N and N-I transitions to be a reversible reaction. The difference of T_{NI} during heating and cooling is small. However, the difference of T_{SN} during heating and cooling is quite large. The result is consistent with the above as more heat is needed to be released to resume back to crystalline from liquid structure during cooling. On heating, the S-N transition is similar to transformation from solid to liquid (e.g. melting) which involves endothermic reaction. But on cooling, the S-N transition is similar to transformation from liquid to solid (e.g. solidification). This involves exothermic reaction. The nucleation of solid phase from liquid phase may require some degree of undercooling to overcome the activation barrier to nucleation of solid phase from the liquid. Therefore, this gives rise to a much lower S-N transition temperature on cooling as compared to heating cycle.

3.1.2 CNTs

MWCNTs were examined by SEM and images were shown in Fig. 3.2. Under low magnification, it can be observed that MWCNTs aggregates into large agglomerations, which consist of a substantial number of individual nanotubes. Under high magnification, it can be seen that MWCNTs are in their typical tubular geometry (length in micro-meter and diameter in nano-meter). Fig. 3.3 shows the Raman spectra obtained with a laser excitation wavelength of 633nm for MWCNTs and the representative D- and G-bands are at the expected peak position. (D = 1347cm^{-1} and G = 1582cm^{-1})[87-90]. Compared with the spectra provided by supplier, it indicates that our sample do contain desired materials and without appreciable amounts of unwanted impurities.

G band (G for graphite) is one of the most important modes of Raman spectroscopy . This mode corresponds to planar vibrations of carbon atoms and is present in most graphite-like

materials[91]. The splitting pattern and intensity depend on the tube structure and excitation energy.

D band (D for defect) is present in all graphite-like carbons and originates from structural defects[91]. It involves the resonantly enhanced scattering of an electron via phonon emission by a defect that breaks the basic symmetry of the graphene plane. This mode corresponds to the conversion of a sp^2-hybridized carbon to a sp^3-hybridized on the surface.

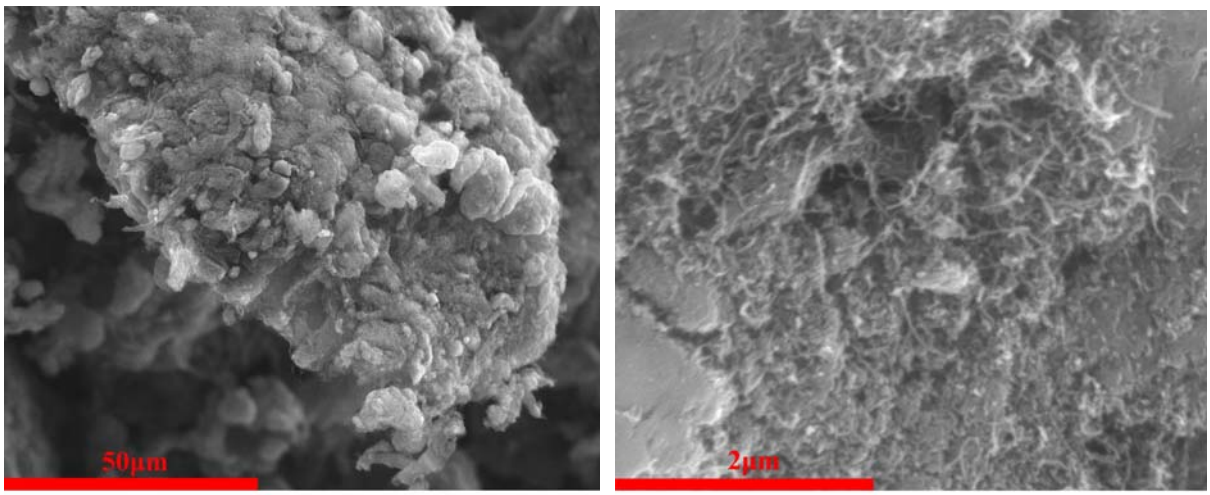

Fig. 3.2 SEM images MWCNTs with magnification of 1000x (left) and 25600x (right)

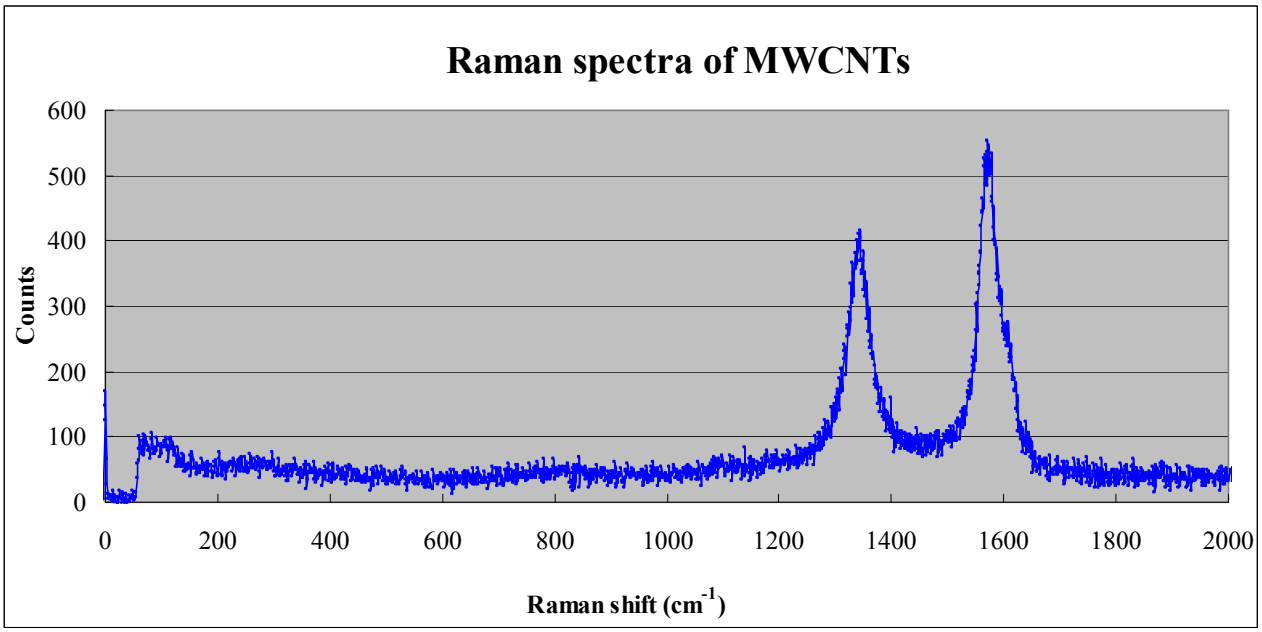

Fig. 3.3 Raman spectra of MWCNTs showing commonly observed D- & G- bands at expected peak positions

3.1.3 LC/ CNTs nanocomposites

After dispersing MWCNTs into the nematic LC host, it was introduced into a LC cell for further investigation. Fig. 3.4 and Fig. 3.5 show polarized light microscopy images of pure LC as supplied and LC with 0.01wt % CNTs (Sonicated at room temperature for one hour without prior stirring) respectively. With the transmitted light, the variation between the on and off states can be observed clearly. For a nematic LC with positive dielectric anisotropy, the external electric field induced Fréedericksz transition from the planar to the homeotropic configuration. As a result, the LCD turns into dark during the on state. In comparison, the images of LC nanocomposite with 0.01wt % CNTs show no significant difference between the pure LC. There is no light leakage during the on state and it implies that MWCNTs follow the LC director during the transition above the threshold voltage (~3V).

With the help of the hot stage, the nematic-isotropic transition can be observed under microscope. Between crossed polarizers the nematic phase exhibits a characteristic bright texture due to its birefringence. When the phase becomes isotropic, it loses its order/ birefringence and the material appears uniformly black. Fig. 3.6 shows the transitions during heating and cooling with a range of 34-36℃ and a scanning rate of 0.5℃/ min. During heating, it can be observed that the birefringence texture is still stable in the proximity of large bundles of CNTs. In contrast, the other area turned black and isotropic phase showed. It indicates that the persistence of the nematic phase in the CNTs bundles area. During cooling, it can be found that the first signs of birefringence appeared around the CNTs bundles. It implies that CNTs bundles act as nucleation centres for liquid crystalline organization and it also confirmed that the LC molecule interact with the CNTs.

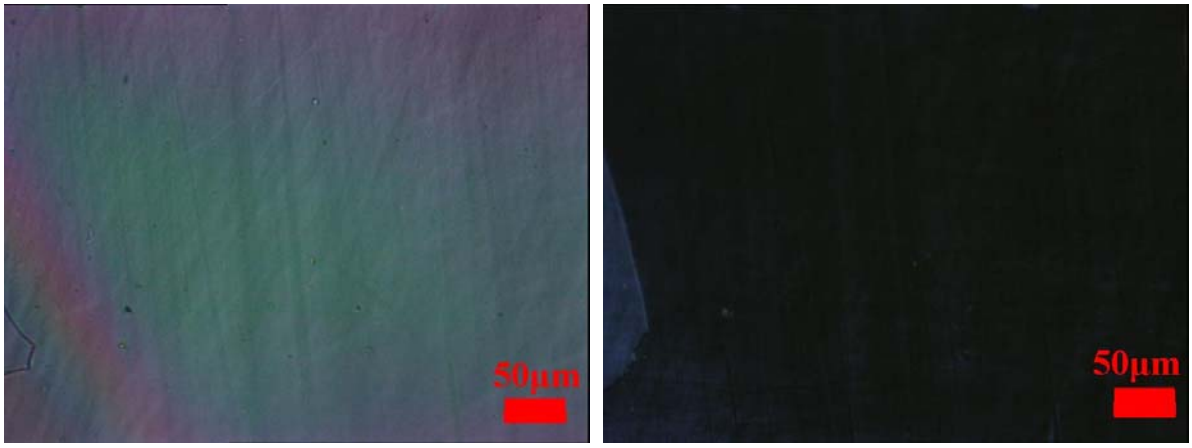

Fig. 3.4 Polarized light microscopy images of pure LC as supplied at the off (left) and on (right) state

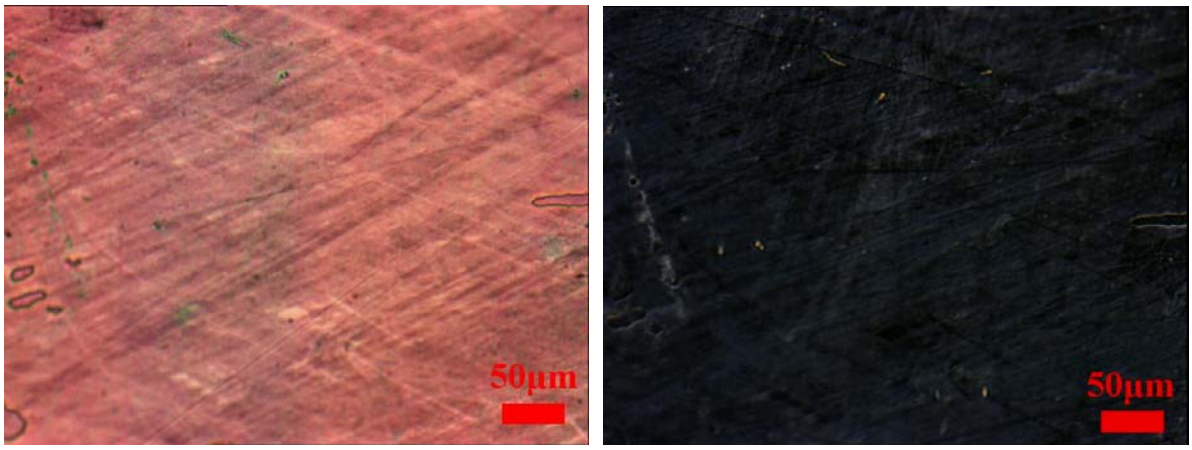

Fig. 3.5 Polarized light microscopy images of LC/CNTs (0.01wt %, room temperature and without prior stirring) at the off (left) and on (right) state

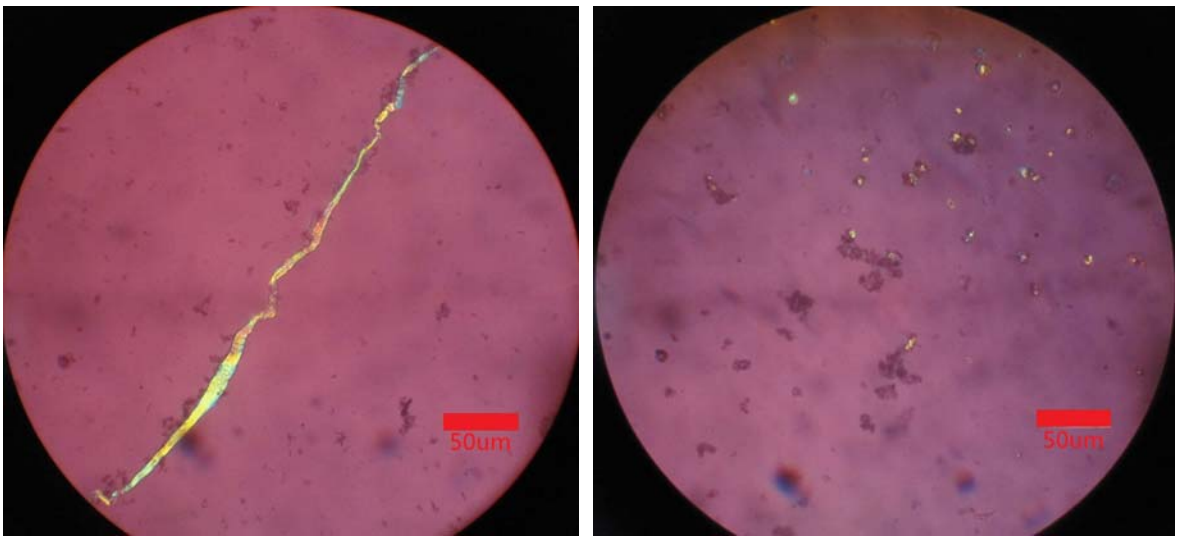

Fig. 3.6 Polarized light microscopy images of LC/CNTs (0.5wt %, room temperature and without prior stirring) during nematic-isotropic transition. Photos of N-I (left) and I-N (right) transitions were taken during heating and cooling respectively

3.2 Dispersion effectiveness

In terms of colloidal dispersion, the term 'stability' often means that there are no signs of phase separation over a period of time or without a tendency to sediment over period of storage. In many practical situations for particles in dispersion, colloid stability implies that the particles have no tendency to aggregate. Therefore, the following studies on the effect of sonication time and temperature on the stability of colloids were performed.

3.2.1 Effect of sonication time

Three samples with same CNTs concentration (0.04wt %) but different sonication time (5, 15 and 30 mins) were prepared to compare the effectiveness of dispersion. Macroscopically observation by naked eyes and microscopically observation by polarized microscope were conducted. Fig. 3.7 shows that the samples before and after centrifugation at 4870RPM

(4000g) with different sonication time. Before centrifugation, sample subjected to 5mins sonication, showed an obvious sign of sedimentation or formation of agglomerates in the liquid mixture. Sedimentation still occurred in samples subjected to 15mins sonication. However, sample subjected to 30mins showed uniform dark color. After centrifugation, all samples were found to be sedimented. But when a closer look was taken, it was found that the suspensions of CNTs in the supernatant are actually in different sizes of the suspended material (Fig. 3.8). By direct observation with naked eyes, the largest one can be observed in sample prepared after 5mins sonication and the smallest suspended particles were found in the sample prepared after 30mins sonication. Polarized microscopy images also confirmed that the size of nanotubes is dependent on the sonciation time as shown in Fig. 3.9. The longer the soication time, the smaller/ shorter the CNTs are. The short sonication time also revealed the agglomeration of CNTs. It obstructs the LCD performance as light leakage can be seen when external voltage is applied (Fig. 3.10). In terms of the observation by naked eyes and microscope, the sample prepared after 30mins sonication was found to be the best as compared to the one with shorter sonication time in this study.

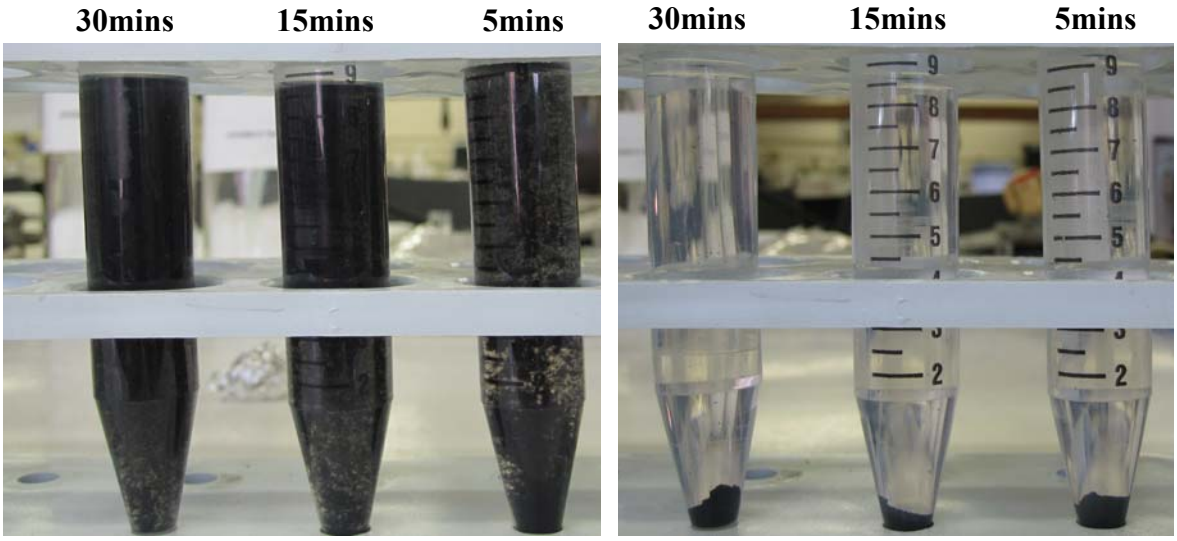

Fig. 3.7 Sample (0.04wt %) with different sonication time before (left) and after (right) centrifugation for 30mins

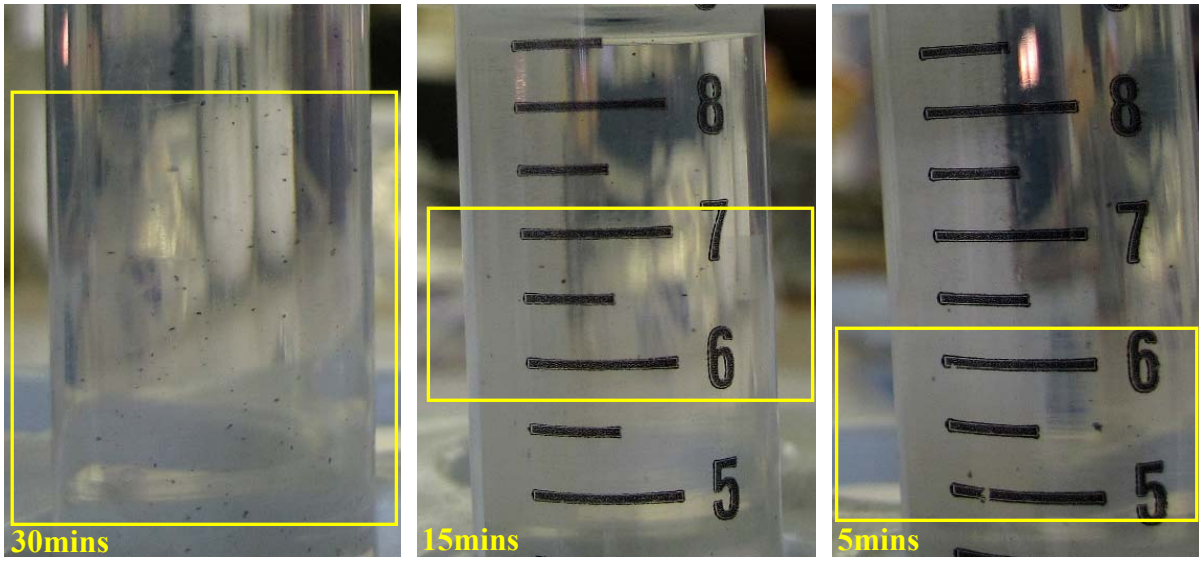

Fig. 3.8 Closer look on the suspensions of different sonciation time after centrifugation for 30mins

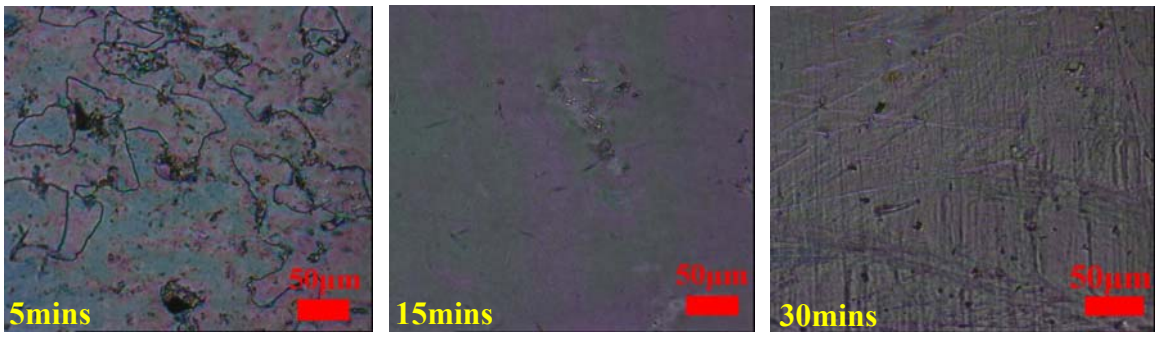

Fig. 3.9 Polarized light microscopy images of different sonication time samples (0.04wt %) at the off state

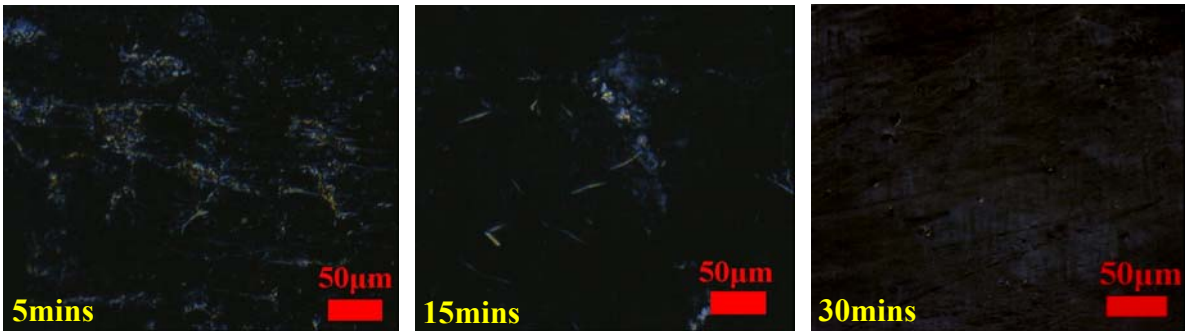

Fig. 3.10 Polarized light microscopy images of different sonication time samples (0.04wt %) at the on state

3.2.2 Effect of 24 hours prior stirring

However, a quite dissimilar picture showed on the samples with 24 hours prior stirring. Fig. 3.11 shows that no entire sediment was found in all three samples after centrifugation for 30mins. The supernatant shows a relatively dark color when it was compared with the one without stirring. Also, the 5mins and 15mins samples exhibited a better dispersion than the 30mins sample. Polarized microscopy also verified that the 5mins sample shown the least CNTs clusters. With the increase in sonication time, the number and the size of the clusters were enlarged (Fig. 3.12 & Fig. 3.13). When external voltage was applied, light leakage is obvious to see on the 15mins and 30mins sample. It implies that dispersion effectiveness is the best on 5mins sonication after a 24 hours stirring.

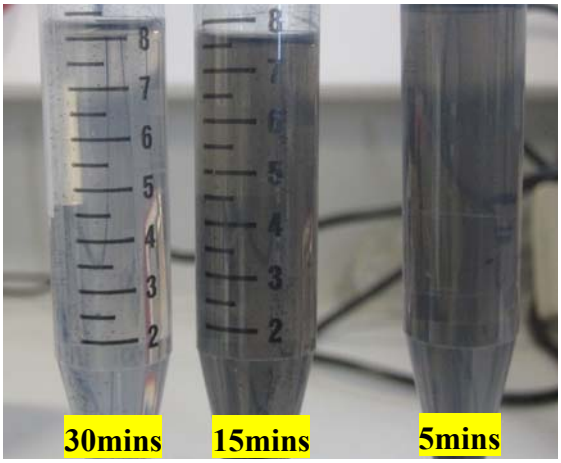

Fig. 3.11 Samples (0.04wt %) with different sonication time and prior stirring after 30mins centrifugation

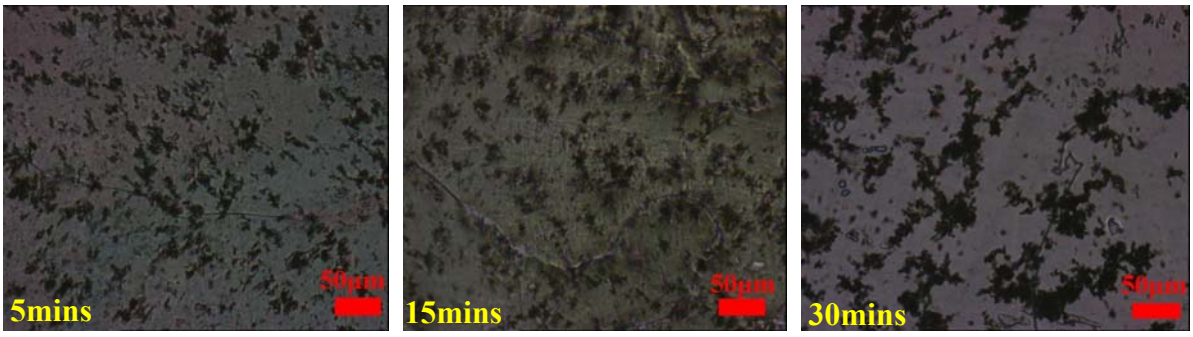

Fig. 3.12 Polarized microscopy images of stirred samples with different sonication time (0.04wt %) at "off" state

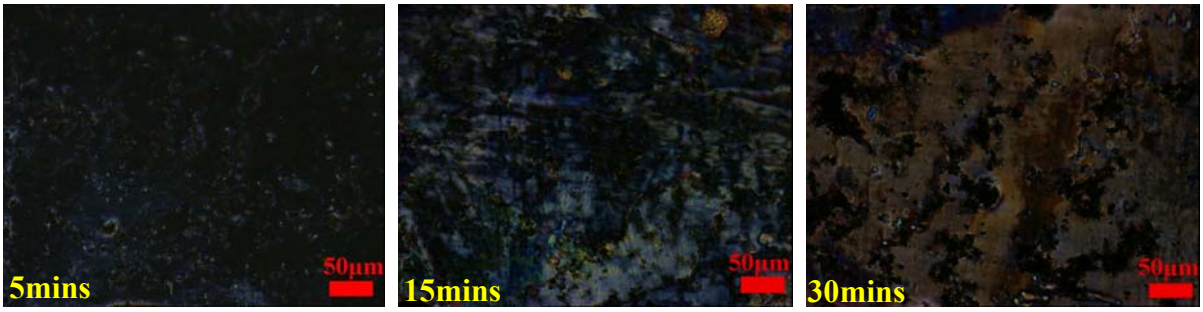

Fig. 3.13 Polarized microscopy images of stirred samples with different sonication time (0.04wt %) at "on" state

3.2.3 Effect of sonication temperature

Due to the mechanical agitation during sonication, the temperature of the medium increases gradually until it reaches certain equilibrium point whether no further increment occurred. Fig. 3.14 demonstrates the relationship between the temperature and sonication time with the measurement of the instant temperature using a thermocouple probe. It was found that the sample temperature rose up to 65℃, which is in the isotropic state of 5CB. To keep the LC material in its nematic state (the area between the two red dotted lines in Fig. 3.14), an ice bath was applied and the temperature was kept at around 28℃ during the whole sonication process. Samples with same CNTs concentration (0.14wt %) but with different temperature treatment were compared under microscope and results were shown in Fig. 3.15. Large-scale CNTs aggregation can be found in the sample treated at room temperature. In contrast, the one soaked in ice bath during sonciation shown relatively small bundles. It is thus clearly advantageous to keep the LC in its nematic phase during dispersion. As shown earlier in the microscopic images, CNTs before sonication are bundle together in which the size is not compatible to the following findings.

With the assistant of image analyzer (ZEISS Axioskop 2), the CNTs diameter distribution in different sociation conditions can be reviewed (Fig. 3.16 & Fig. 3.17). As shown clearly in the

figures, a wider distribution can be seen in the graph of the CNTs sonicated in room temperature. The peak also shifted to the increasing diameter of CNTs. With the confirmation of the average value from the CNTs counted in the microscope photos with the image analyzer (pink line in the graph), it is obvious to see that the average sizes of the sample sonicated in the room temperature are larger than the one sonicated in ice bath. (Average sizes for room temperature and ice bath are 5.16 arb.unit and 4.03 arb.unit respectively. Size reduction is 22% for sonication in ice bath). Both microscope observation and image analyzer results concluded that ice bath is beneficial to reduce CNTs bundles during sonication.

Remarks: The arbitrary unit in Fig.3.15 is with the same scale in the image analyzer software.

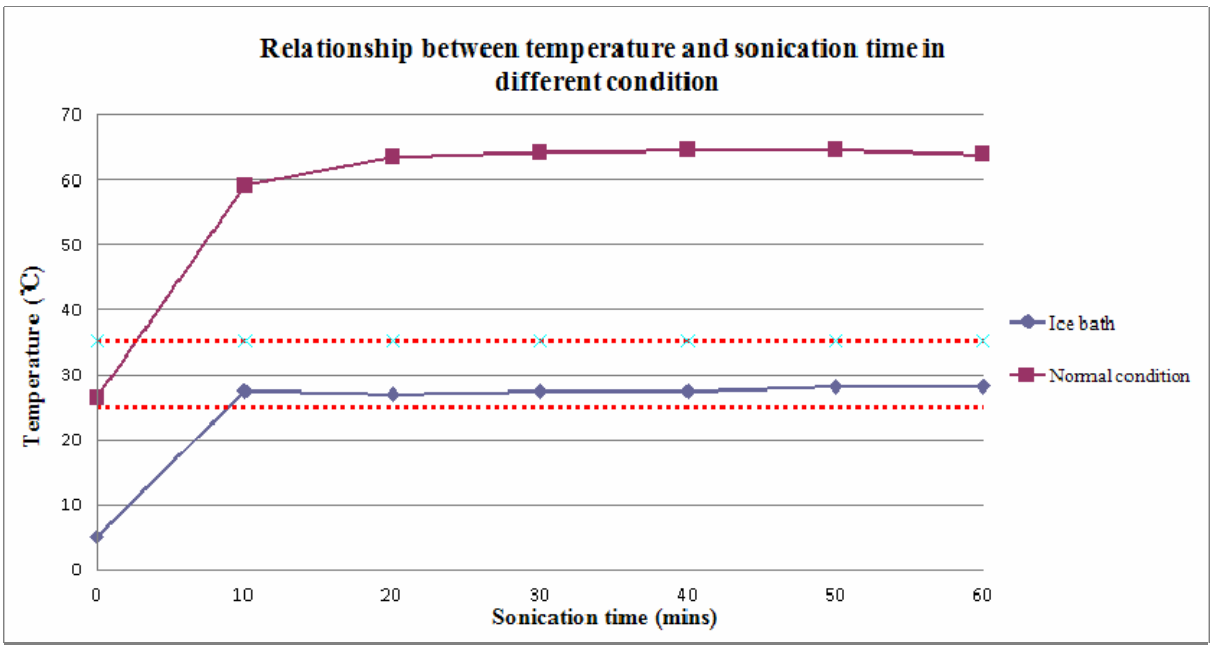

Fig. 3.14 Relationship between temperature and sonication time in normal condition and ice bath

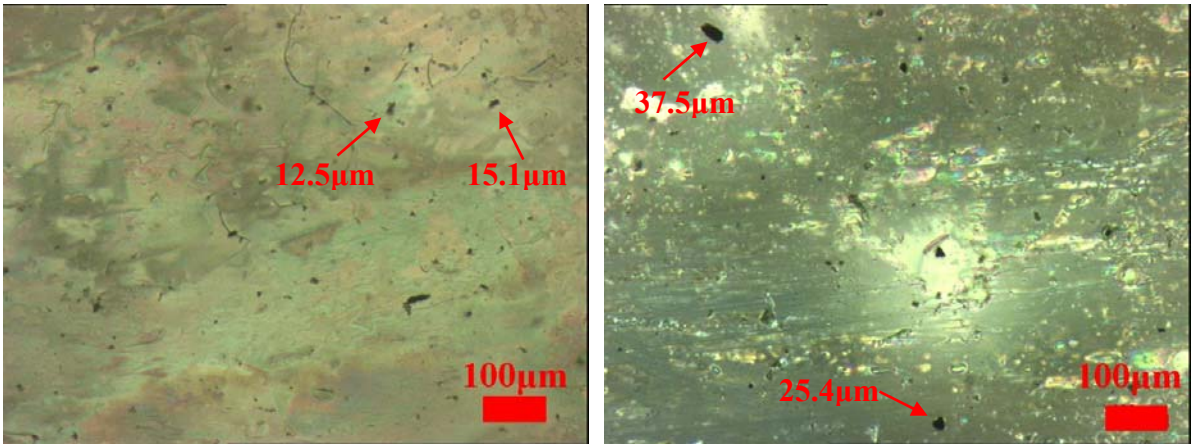

Fig. 3.15 Polarized light microscopy images of 0.14wt % CNTs LC composites treated in ice bath (left) and at room temperature (right)

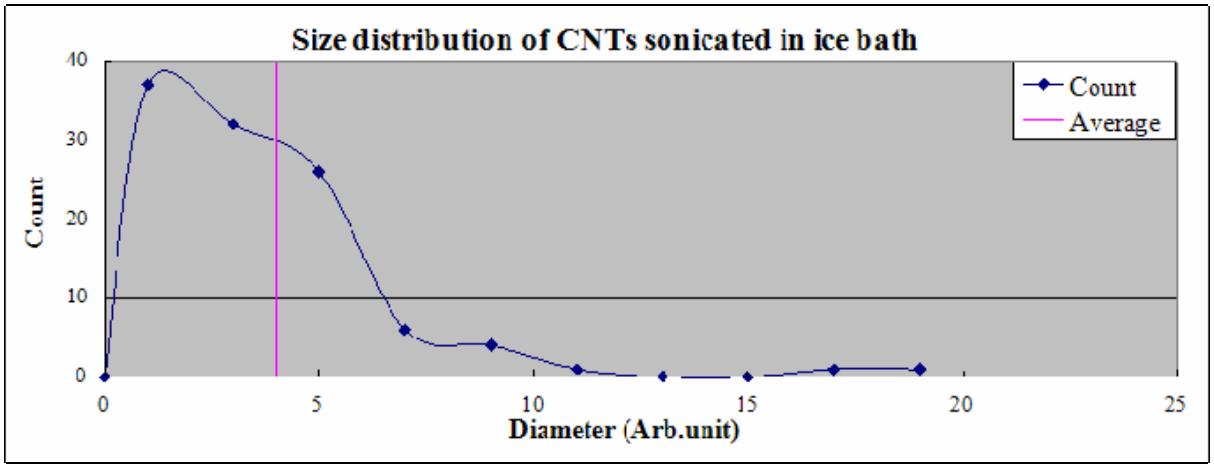

Fig. 3.16 Size distribution of CNTs (sonicated in ice bath without prior stirring) obtained by image analyzer of 0.14wt % CNTs LC composites

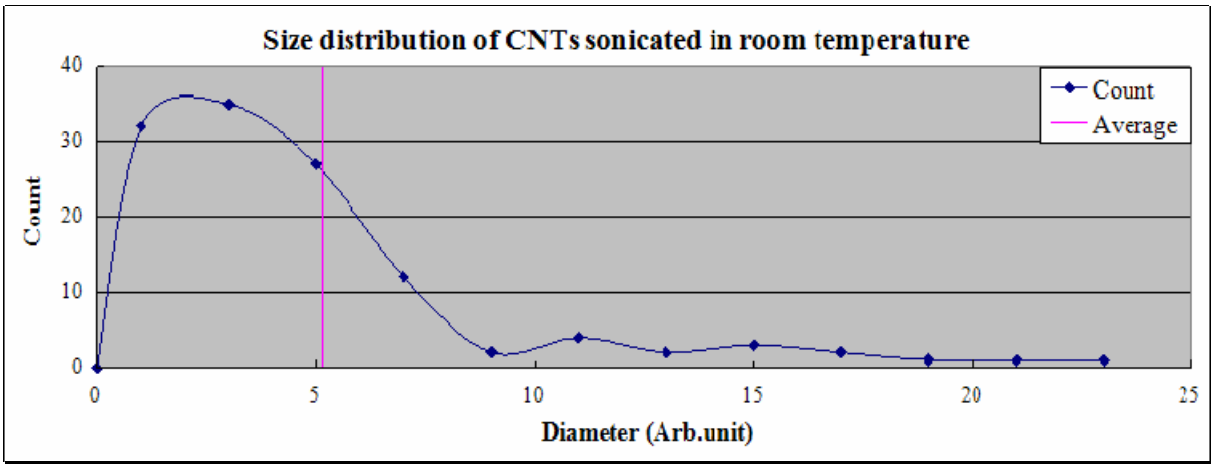

Fig. 3.17 Size distribution of CNTs (sonicated in room temperature without prior stirring) obtained by image analyzer of 0.14wt % CNTs LC composites

3.2.4 Effect of CNTs concentration

The concentration of the nanoparticles plays a very important role in the LC nanocomposite system. Fig. 3.18 and Fig. 3.19 show the on and off state of 0.01wt %, 0.05wt % and 1wt % under polarized microscopy respectively. Samples were sonicated at room temperature and

without prior stirring. For low concentration of 0.01wt%, CNTs were uniformly distributed in LC and no bundle was found. When the CNTs content was increased, the number of CNTs clusters started to increase and finally large bunches of nanotubes were found in the 1wt % sample. Serious light leakage was found in large CNT agglomerates, when the LCD cell was turned on. This indicates that high concentration of CNTs degrade the LCD performance.

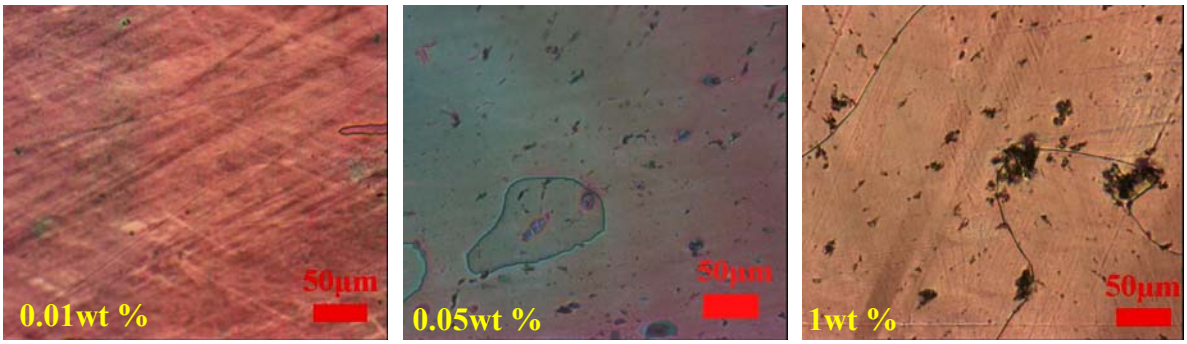

Fig. 3.18 Polarized microscopy images of different CNTs concentration samples at "off" state

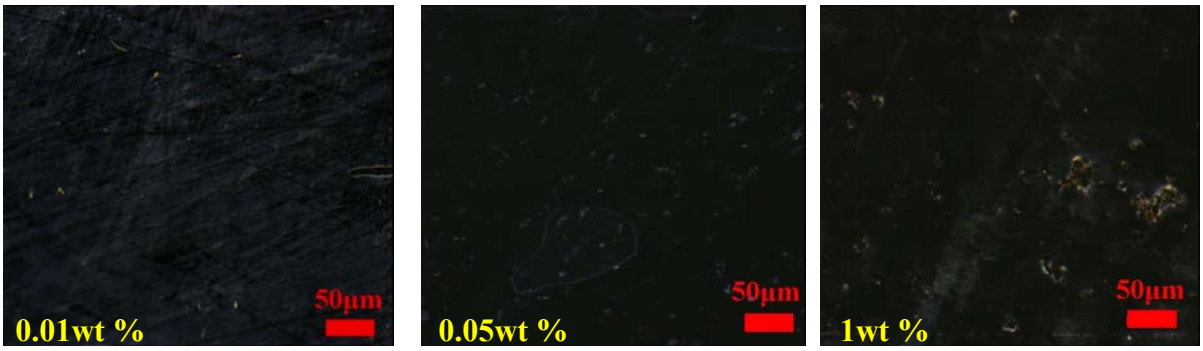

Fig. 3.19 Polarized microscopy images of different CNTs concentration samples at "on "state

In order to have a deeper understanding of the LC/ CNTs interaction, calorimetry experiment on different CNTs concentration was conducted. The temperature range of -20°C to 50°C and a scanning rate of 5℃/ min were used in this study. A slightly change in the nematic-isotropic transition temperature (T_{NI}) during both heating and cooling cycles was found as shown in Table 3.1. In both cases, the temperature decreased slightly when small amount of CNTs were added (Maximum variation is 0.23℃ for heating and 0.25℃ for cooling). However, as the concentration reached to 0.5wt % or above, the T_{NI} temperature was higher than pure LC

(0.14℃ higher for heating and 0.2℃ higher for cooling). The relationship between the transition temperature and the CNTs content was plotted in Fig. 3.20. Tests were repeated twice to ensure the consistency of the transition temperature of each concentration of CNT. It can be observed that the trends of heating and cooling cycles are almost identical to each other.

CNTs wt%	T_{NI} (Heating)	T_{NI} (Cooling)
Pure LC (0wt % CNTs)	35.26℃	34.07℃
0.01wt % CNTs	35.27℃	33.98℃
0.02wt % CNTs	35.18℃	34.02℃
0.05wt % CNTs	35.03℃	33.82℃
0.14wt % CNTs	35.15℃	33.92℃
0.5wt % CNTs	35.32℃	34.23℃
1wt % CNTs	35.40℃	34.27℃

Table 3.1 Nematic-isotropic transition temperatures (T_{NI}) with different CNTs concentration during heating and cooling

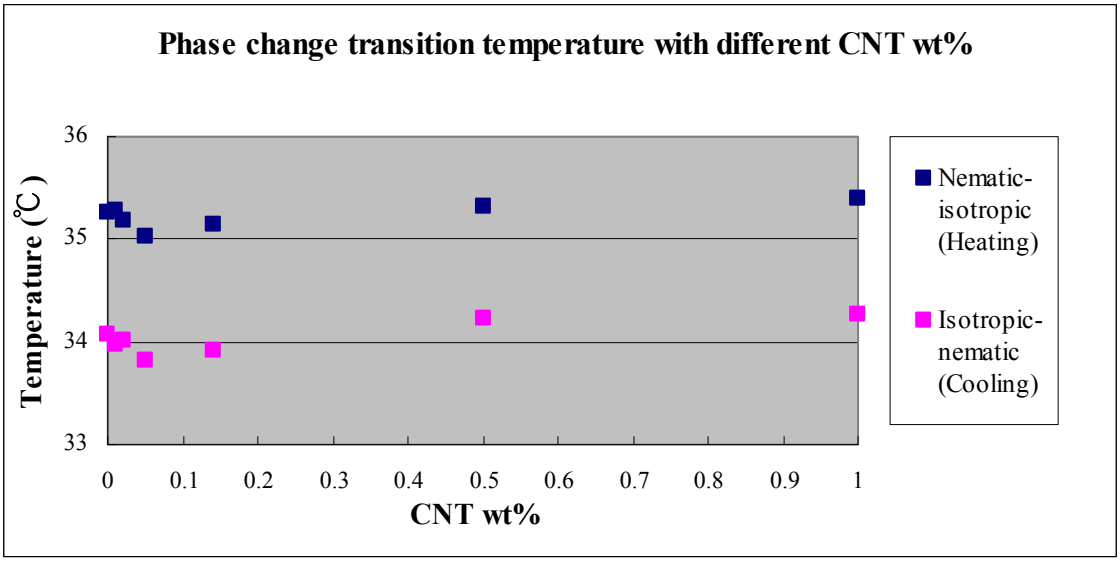

Fig. 3.20 Trends of T_{NI} with respect to different CNTs wt%

3.3 Electro-optical (EO) behavior measurement

This section presents the results on the EO performance of LCDs. Threshold voltage and

response time are critical concerns for a LC device. Low threshold voltage and fast response time result in a better performance for the optical device because lower power consumption can be achieved by lower threshold voltage. Faster switching time allows the application in more complex display technologies like 3D TVs.

3.3.1 Effect of sonication time

As shown in below again, the typical on-off switching graphs (Both brightness vs operating voltage and brightness vs time) were illustrated in section one. (Fig. 1.10) For the LCD configuration of the samples used in this project, the brightness is 100% when there is no voltage applied. However, the brightness decreases with increasing applied voltage and eventually reaches to a 0% brightness level. The rise time or fall time is defined as the time when the brightness changes from 10% to 90% or 90% to 10% respectively.

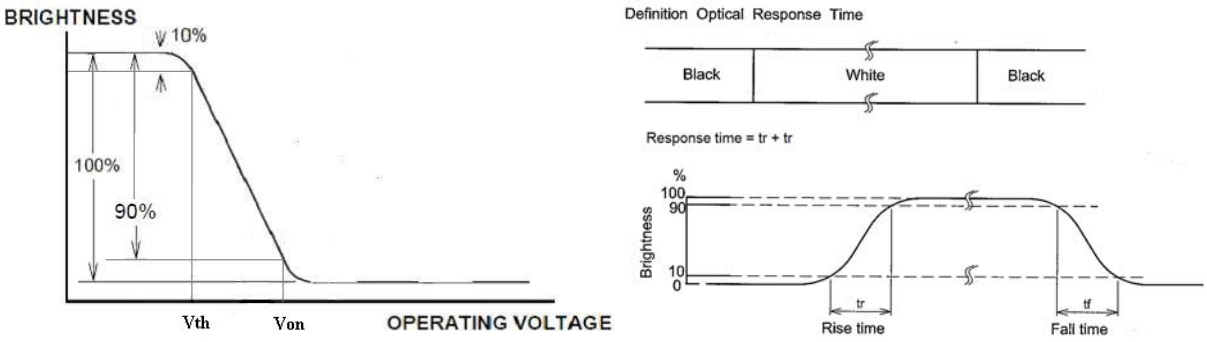

Table 3.2 gives a summary of the field on time, field off time, total response time and threshold voltage as a function of sonication time. It was found that field on time, field off time, total response time and threshold voltage decreased with increasing sonication time. With respect to section 3.2.1, the EO performance was related to the size of the aggregation. The 30mins sample achieved the smallest size of bundles under the examination of

microscope. In terms of EO performance, it also performed the best among the three.

Sonication time	Field ON time	Field OFF time	Total response time	Threshold voltage (V_{10})
5mins	199.3ms	210.7ms	410.0ms	3.50V
15mins	127.9ms	179.2ms	307.1ms	3.32V
30mins	87.5ms	175.0ms	262.5ms	3.09V

Table 3.2 EO performance of 0.04 wt % CNTs LCD cells with different sonication time (Sonicated at room temperature and without 24 hour prior stirring)

3.3.2 Effect of 24 hours prior stirring

However, with 24 hours stirring prior to sonication treatment, the results were totally different to the one from above. Table 3.3 gives a summary of field on time, field off time, total response time, threshold voltage as a function of sonication time. All the EO characteristics for samples prepared with 24 hours stirring prior to sonication gave an increasing trend with increasing sonication time. The best EO characteristics were found in sample prepared using 24 hours stirring prior to 5mins sonication at room temperature. This is correlated with the smallest sizes of particles in the CNT/LCD suspension as presented in section 3.2.2. It reflects that the size of CNTs in the LC host is critical to the LCD performance.

Sonication time	Field ON time	Field OFF time	Total response time	Threshold voltage (V_{10})
5mins	35.4ms	108.4ms	143.8ms	2.57V
15mins	81.5ms	180.9ms	262.4ms	3.91V
30mins	281.9ms	432.5ms	714.4ms	4.39V

Table 3.3 EO performance of 0.04 wt % CNTs LCD cells with different sonication time and 24 hours prior stirring (Sonicated at room temperature)

Fig. 3.21 shows the comparison of EO characteristics between the 0.04wt% CNTs samples with and without stirring. For the 5mins sonciation time, the stirred one exhibits better EO characteristics than the one without stirring. The one without prior stirring performed the best when the sonication time is 30mins. But if the 5mins sonication with prior stirring sample and 30mis soication without prior stirring sample were put together, the 5mins sonication with prior stirring sample was by far the best. It reviewed that prior stirring is effective to achieve better LCD performance. But prolonged sonication may lead to the degradation as well.

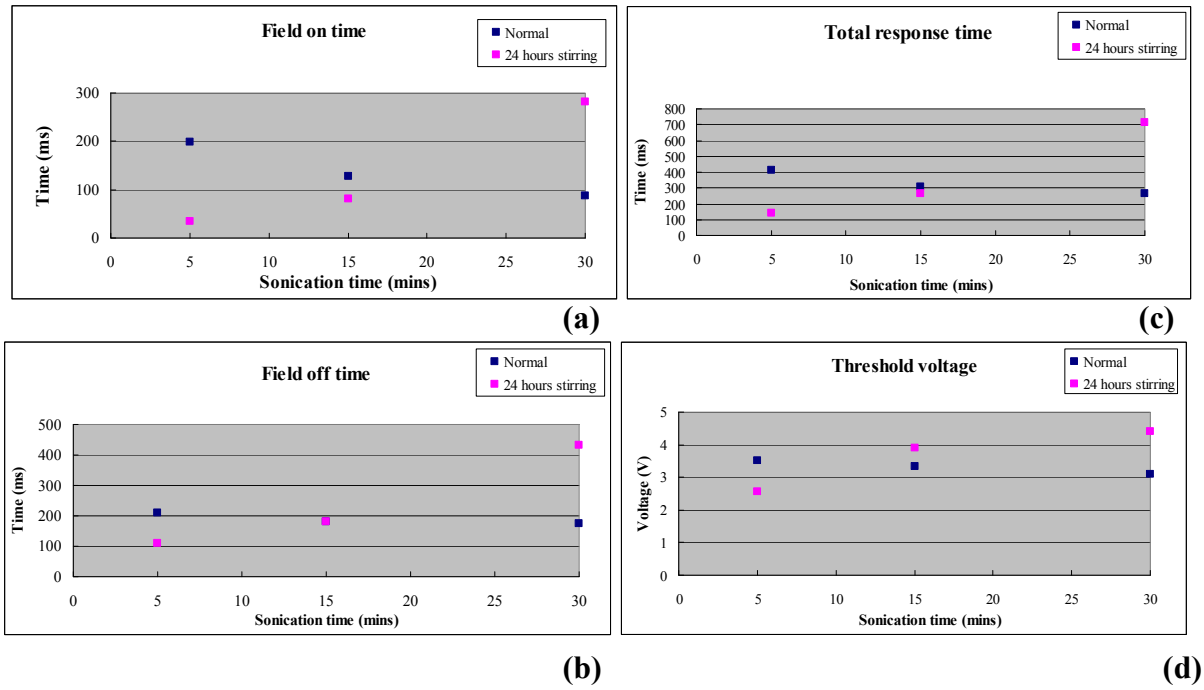

Fig. 3.21 Summarized EO performance between sample (0.04wt %) with and without stirring at different sonication time: (a) Field on time (b) Field off time (c) Total response time and (d) Threshold voltage

3.3.3 Effect of sonication temperature

Table 3.4 and Fig. 3.22 show the LCD switching behavior of LCD cells with different CNTs concentration and sonication temperature. With the same concentration, the sample sonicated

under ice bath performed better than the one under room temperature. The ice bath samples achieved faster response time and smaller threshold voltage. Refer to section 3.2.3, mechanical power produces heat during sonication and LC materials transformed from nematic state to isotropic during the process. Ice bath is effective to resist the raise of temperature and keep LC materials in the self organized nematic state. From the results, the EO features were obviously beneficial to keep LC in its nematic state during dispersion.

Condition	Field ON time	Field OFF time	Total response time	Threshold voltage (V_{10})
0.01wt % CNTs	35.0ms	490.0ms	525.0ms	2.30V
0.01wt % CNTs Ice bath	35.8ms	459.9ms	495.7ms	1.36V
0.14wt % CNTs	56.9ms	142.4ms	199.3ms	2.78V
0.14wt % CNTs Ice bath	93.3ms	105.0ms	198.3ms	2.43V
1wt % CNTs	102.5ms	550.0ms	652.5ms	5.01V
1wt % CNTs Ice bath	96.6ms	489.7ms	586.3ms	4.55V

Table 3.4 EO features corresponding to different CNTs concentration and sonication temperature

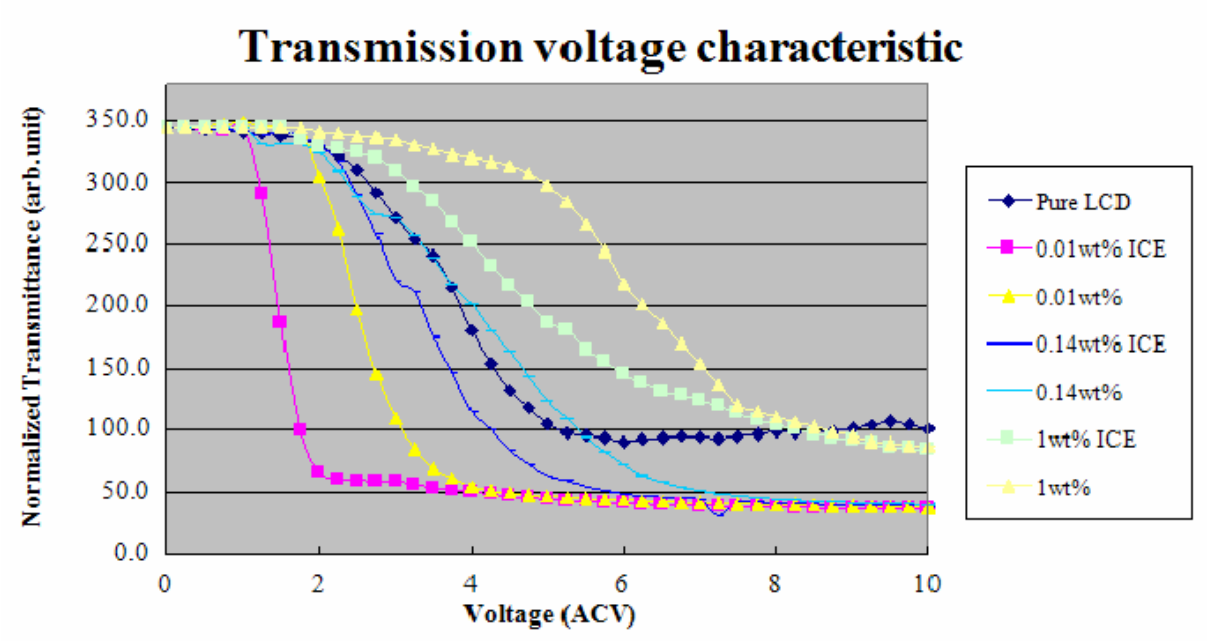

Fig. 3.22 Transmittance as a function of AC voltage with different CNTs wt% & sonication temperature

3.3.4 Effect of CNTs concentration

Table 3.5 and Fig. 3.23 showed the LCD switching behavior of LCD cells with different CNTs concentration. The samples were sonicated under room temperature condition and without any prior stirring. For response time, it increased on the 0.01wt % sample and then decreased gradually with increasing CNT concentration. When the CNTs concentration increased above 0.5wt %, the switching behavior was worse than those of pure LC sample. In terms of threshold voltage, samples below 0.05wt % performed better than pure LC one. However, the sample with 0.14wt % CNT, gave similar EO performance as pure LC. Again, the Vth of 0.5wt % samples or higher is larger than the pure one. Overall, the 0.02wt % sample achieved the best results and it was believed that it is the optimal concentration for this 5CB/ MWCNTs hybrid system.

Condition	Field ON time	Field OFF time	Total response time	Threshold voltage (V_{10})
Pure LC (0wt % CNTs)	51.3ms	227.8ms	279.1ms	2.63V
0.01wt % CNTs	35.0ms	490.0ms	525.0ms	2.30V
0.02wt % CNTs	56.9ms	142.4ms	199.3ms	1.97V
0.05wt % CNTs	45.6ms	148.1ms	193.7ms	2.13V
0.14wt % CNTs	56.9ms	142.4ms	199.3ms	2.78V
0.5wt % CNTs	85.5ms	336ms	421.5ms	3.8V
1wt % CNTs	102.5ms	550.0ms	652.5ms	5.01V

Table 3.5 EO features corresponding to different CNTs concentration

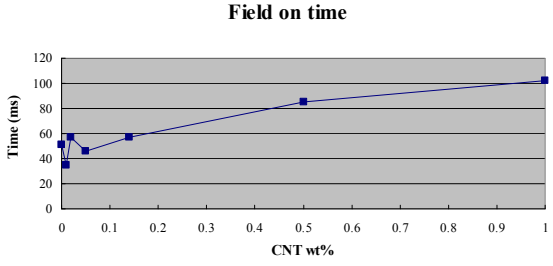

(a)

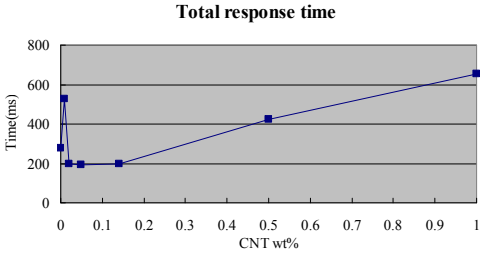

(c)

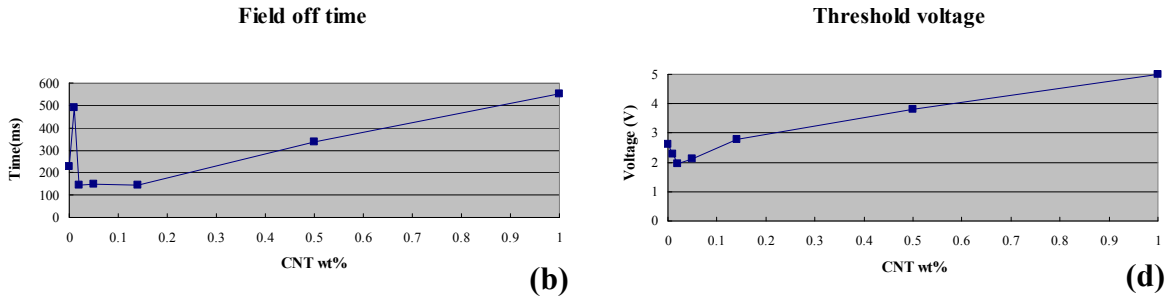

Fig. 3.23 Summarized EO performance between sample with and without stirring at different CNTs concentrations: (a) Field on time (b) Field off time (c) Total response time and (d) Threshold voltage

Fig. 3.24 showed the graph of optical transmission against time during electrical switching with different CNTs concentration. It was clear to see the backflow effect (oscillation right after the voltage is switched off from the on state) on the pure LC sample. When the CNTs content is at 0.01wt %, the backflow was slightly suppressed. At 0.02wt %, the light rise rapidly without oscillating and the backflow effect was regarded as disappeared. However, when the CNTs concentration is high as 1wt %, the backflow occurred again and lowered the response time.

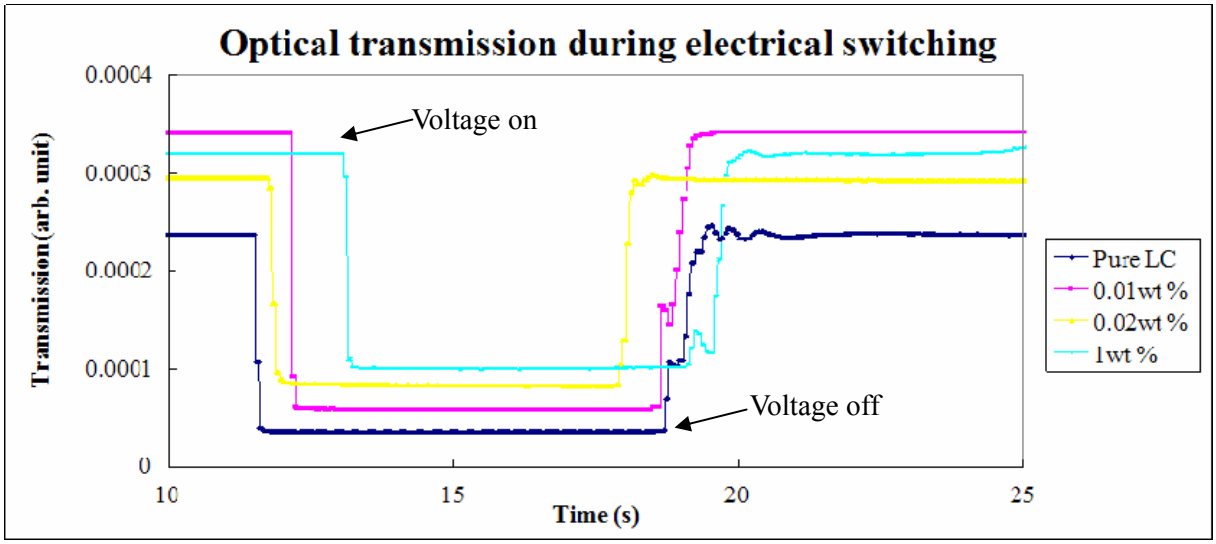

Fig. 3.24 Optical transmission upon electrical switching of pure LC, 0.01wt % CNTs, 0.02wt % CNTs and 1wt % CNTs

4. Discussion

4.1 Effect of sonication time

Sonication under ultrasonic wave is an effective way to obtain a better dispersion for agglomerative nanoparticle like CNTs. During storage, CNTs form aggregation and this lowered its solubility in other medium. Sonication provided mechanical agitation to break the bundles to increase CNTs' integrity of the whole system and the duration is critical to the CNTs bundles' size. To achieve a uniformly dispersed CNTs suspension, longer sonication time is necessary and this can prevent the aggregation of the CNTs inside the solution. Insufficient and prolong sonication time leads to large CNTs clusters in the LC host and causes light leakage when voltage is applied to the LCD cell. Other EO features such as response time and threshold voltage were also obstructed by the clusters.

Other than that, additional strategies were used to enhance the dispersion effectiveness. The first one is the selection of polar aprotic solvents such as DCE. The dispersant counteracts the van der Waals attraction of adjacent CNTs by introducing sufficiently strong repulsive force between them. The second one is the usage of COOH functionalized MWCNTs and it is believed that the surface modification of nanotubes enhanced the compatibility of the whole system. The acid treatment introduces oxygen-containing functional groups onto the surface to give a negatively charged surface. The resulting electrostatic repulsive forces enrich the dispersibility and stability of the colloidal.

To sum up, chemical functionalization, ultrasonication and the use of surfactant are ways to promote the dispersion in a satisfactory way through debundling and counteracting the reaggregation. However, it is also important to note that undesirable addition to the host may potentially be existed and this amount of impurities should be limited. In some occasions with improper matching between chemicals and CNTs, unexpected reactions or undesired solvent effect may undergo and it will affect the intrinsic properties of the CNTs.

4.2 Effect of 24 hours prior stirring

Ultrasonication is quite essential for good dispersion. Though, the results with 24 hours prior stirring did not reflect the same. With prior stirring, the shortest sonication time (5mins sample) achieved the best performance. When sonciation time increases, the number of agglomerations also increased. In terms of the observation of microscope images and EO performance, the best dispersions are those that had been stirred followed by a brief sonication (5 mins) because it obtained an uniform distribution in microscopic observation and achieved the best EO performance.

Prior stirring gives mechanical power and breaks the CNTs into smaller bundles before ultrasonication. As you can see from the microscope images in section 3.2.2, more uniformly distributed CNTs can be found in the 5mins sample with prior stirring than the one without it. This reflected that prior stirring is advantageous to homogeneous dispersion of CNTs in 5CB. But as the sonication time increases, the LCD cell performance degrades. As seen from the 15mins and 30mins sonication samples, prolonged sonication does not necessarily improve the dispersion but can in fact have the opposite effect. Due to the increased chance of contact between particles, it is well known that colloid aggregation can be induced by shear flow[22]. It can be concluded that during the preparation of colloids dispersion, there is thus a trade-off between the reduction of the particle size achieved by mechanical processing and the increased risk of aggregation. This may varies from the combination of different LC materials and nanoparticles as well.

4.3 Effect of sonication temperature

It was found that the microscopic structure of the LC material has a dramatic impact with different sonication temperature. Keeping the LC host in its nematic phase during sonication is beneficial for preparing the dispersion as well as for maximizing the stability. In other word, heating the LC material

above its clearing point decrease the dispersion effectiveness (where it turns into an isotropic liquid). For long term stabilization of the nanocompsites, it is better to store it in the nematic phase, rather than the isotropic phase.

The long range orientational ordered nature of LC materials help to keep the dispersion in a stable state. Experimental results showed that the average size of agglomerations in the isotropic state is larger than the nematic state and it confirmed that the importance of anisotropic properties of LC materials. The ordered structure resists the formation of CNTs cluster. In contrast, CNTs are randomly distributed and clusters are formed more easily in the isotropic state. In addition, agitation with considerable heat often induces clustering and sedimentation of the suspended CNTs, which is another reason why it is beneficial to keep the mixture into ice bath during sonication. It is also noted that the viscosity variation in the temperature range investigated is small (The viscosity of 5CB at room temperature and 50°C are 22.5mPa.s and 21.5mPa.s respectively[92]) and the viscosity reduction did not contribute to the reduced stability of the isotropic samples.

By considering the Gibbs free energy of mixing:

$$\Delta_{mix} G = \Delta_{mix} H - T\Delta_{mix} S$$

where $\Delta_{mix} H$ and $\Delta_{mix} S$ are the enthalpy and entropy related to the mixing process respectively and T is the temperature.

Dissolution of a solute in a solvent is favorable to take place if $\Delta_{mix} G$ is negative. The dissolution of CNTs is challenging because carbon nanotubes are extremely long and stiff rod and $\Delta_{mix} S$ is exceptionally low. In order to promote good dispersion, solvent must interacts favorably with nanotubes such that $\Delta_{mix} H$ is negative. Molecular properties like aromaticity, high polarizability, and strong dipole moment are favor to the interaction with CNTs and LC materials are actually quite promising as CNTs host due to the low$\Delta_{mix} H$ value.

During sonication, the configurational entropy of solvent molecules decreases because they were absorbed by the rapidly expanding area of exposed CNTs surface. This solvation entropy penalty can increase Δ_{mix} G substantially[93]. In the nematic phase, LC is itself ordered and it should make the solvation entropy less pronounced. The absorption of mesogns onto CNTs introduces a positional order that is not present in a nematic phase and hence the entropy loss due to adsorption-induced alignment is negligible. On the other hand, in the case of isotropic phase, this would constitute a severe additional entropy decrease. So, keeping the solvent in its nematic state thus minimizes the solvation entropy and makes the mixing more desirable. This is also supported by other study on LC wetting of HOPG[94] (Highly Ordered Pyrolitic Graphite) and it demonstrated that LCs generally wet HOPG in the nematic but never in the isotropic state.

The ordered property of nematic solvents also gives unique enthalpy contributions. Disordered nanotube aggregates in the nematic phase distort the director field strongly on a small scale. In contrast to the case of isotropic liquids, which cannot take up elastic stresses, the presence of CNTs aggregates in a nematic host is thus connected to an elastic energy penalty, i.e., the aggregates increase Δ_{mix} H. The impact will be smaller for smaller aggregations, being essentially zero in case of bundles of uniformly oriented tubes, hence the free energy can be minimized by dissolving large random aggregates. This should contribute to the reduction in aggregate size during dispersion in nematic solvents as well as increase the dispersion stability in case good debundling has been achieved.

4.4 Effect of CNTs concentration

First of all, let us focus on the influence on the LC transition temperature with different CNTs concentrations. When the CNTs concentration is low, the transition temperature T_{NI} is lower than or more less the same as the pure LC. This may be due to the large heat dissipation of the highly thermal conducted CNTs. However, when the concentration went up to 0.5wt % or higher, T_{NI} is larger than pure LC. It is likely because the formation of heterogeneous nucleation when the carbon content is high. The DSC curves suggest that the large scale structure formed in the LC after its filling with MWCNTs do not completely disappear at the nematic-isotropic transition temperature. In addition, a complex structure of the transition peaks is observed for the composites. These data reflect the structural heterogeneity of the composites and may be the evidence of the presence of spatial regions with different structural ordering of the LC.

Because CNTs have extraordinary thermal conductivity, heat can be withdrawn very fast from a source. When the CNTs/ LC nanocomposites are heated up, CNTs bundles start to dissipate the heat and the temperature around the bundles should be lower than the other area. That is the reason why the birefringence texture is still observable in the proximity of large bundles of CNTs. Also, this is the explanation for lower T_{NI} when the CNTs concentration is low because heat is dissipated during the phase transition.

In general, there are two nucleation paths for a material under heating and cooling cycle. Nucleation normally occurs at nucleation sites on surfaces or at grain boundaries. Though, suspended particles or minute bubbles also provide nucleation sites and this is called heterogeneous nucleation. Nucleation without preferential nucleation sites is called homogeneous nucleation. Homogeneous nucleation occurs spontaneously and randomly, but it

requires superheating or supercooling of the medium. By the microscopic observation with hot stage, it can be found that agglomerations acted as nucleation sites and heterogeneous nucleation took place in the CNTs/ LC nanocomposite transition. During cooling cycling with high CNTs concentration, the nucleation starts at the CNTs bundles and propagate to other area. Whereas, for pure LC, homogeneous nucleation took place as there is no nucleation site. To start the nucleation, supercooling is required and a lower temperature is needed to obtain the first nucleation site. As a result, the T_{NI} of pure LC is lower than the one with high CNTs concentration.

In theory, non CNTs impurities may affect the microstructural performance during phase transformation. But from the test results, this kind of impurities seems did not contribute much in the heating and cooling process. In heating process, impurities did not dissipate heat as fast as CNTs so that we can only observe LC nematic state around CNTs bundles. In cooling process, supercooling was observed instead of impurities act as nucleation sites. This may be explained by the low concentration of impurities within the hybrid system.

For the EO performance, CNTs concentration plays an important role on the display switching behavior. By doping CNTs into LC host, the backflow effect was effectively suppressed. In addition, the threshold voltage and response time were improved. In terms of the overall display performance, the optimal CNTs concentration for 5CB/ MWCNTs nanocomposites of this study is 0.02% wt.

By referring to Equation 1.1, threshold voltage is a function of the elastic constants and inversely proportional to the square root of the dielectric anisotropy $\Delta\varepsilon$. In theory, the elastic constants will increase with increasing CNTs concentration. But because the amount of additives is very small, the change in the three elastic constants is insignificant. In contrast,

the high aspect ratio CNTs has large Δε and this result in the substantial decrease in $V_{th.}$ Other study also demonstrated the remarkable increase in Δε with higher CNTs content[7]. Nevertheless, when the CNTs concentration is relatively high (>0.5% wt), V_{th} became larger than the one of pure LC. This is mainly attributed to the formation of CNTs aggregation which obstructed the switching ability of the LC molecule and decreased the Δε.

The faster response time on the nanocomposite is related to the decrease in rotational viscosity. Refer to Equation 1.2 & 1.3, the rise time and fall time are directly proportional to visco-elastic coefficient (The ratio of the rotational viscosity to the elastic constant, γ_1 / K_{ii}) and cell gap d. To shorten the response time, thinning the cell gap is a straightforward approach. But when the cell gap is small, the uniformity of the alignment layer thickness and surface roughness become important. Moreover, the reduced cell gap often leads to a low contrast ratio of the device owing to the insufficient phase retardation. And in the real mass production line, it is challenging to make thin cell panels with acceptable yield and quality. Because of the reasons mentioned above, more emphasis was put into the methods to lower the rotational viscosity of the LC material and doping CNTs is one option. In this study, the cell gap was under controlled at a relatively stable value which should not contribute to the change in response time. Though, the variation in response time with different CNTs is attributed to the decrease in rotational viscosity. From the data of other study, it was believed that the rotational viscosity is lower in the suspension than that for the host material and it was found to vary monotonically with the concentration of CNTs[4]. The possible mechanism behind may be explained by the difference in rotational velocity between the pure LC and the dopant in the dilute colloid. When voltage is applied to the CNTs doped cell, LC molecules and CNTs experience a torque in different magnitudes because their aspect ratio and dielectric anisotropies are not the same. This also revealed that the electric dynamic responses are not the same in the neat and doped cell. The incoherent responses suppress the collective behavior

of LC molecules and possibly result in a decrease in rotational viscosity.

When the CNTs concentration is high, the response time increases and the switching behavior is worst than the pure LC material even the rotational viscosity is further reduced. This contradicted behavior can be explained by the change in ion concentration with different CNTs contents.

High ion contamination is always a problem for LCD industry. The absorbed charge at the interfaces between the alignment layers and LC layer reduces the effective electric field across the cell and diminishes the polarity of the external field. This leads to image-sticking problem in which the birefringence remained when the applied voltage is off. Some researchers measured the value of ion concentration with respect to different CNTs content[4] and it obviously showed that the ion concentration is higher than pure LC in the 0.1wt % CNTs sample. Because of the higher ion concentration, image-sticking effect occurred and perturbed the switching behavior of the cell and result in a longer response time.

The response time of the best cell (0.02% wt) is much larger than the commercial LCDs in the market. This can be explained by the difference in the LCD cell production feasibility between the lab and production line. Facilities limitation, environmental imperfection and processing restriction etc. are the negative effects of longer response time of the LCD cell prepared in the lab. This implies that the data in the research may not be a good reference to the commercial ones. Nevertheless, all the LCD cells prepared in the lab are under similar process and environmental conditions and the data obtained is compatible to express the effect of CNTs dopants.

5. Conclusions and outlook

In this report, LC/MWCNTs hybrid material was studied. Characterizations of both individual materials and the hybrid system were conducted. Also, to obtain better integrity, sonication was done and the corresponding parameters were considered to compare the dispersion effectiveness. Furthermore, LCD cells were fabricated to evaluate the EO performance with different sonication parameters and CNTs concentrations.

From DSC studies, the two transformation features of LC material were showed. From SEM studies, the disordered nature of CNTs can be observed. When the two materials mixed together, interaction can be found. With the help of microscope, it can be seen that MWCNTs follow the LC director when the CNTs concentration is low. There is no light leakage when an external voltage is applied. With the assistance of the hot stage, the microscopic view during the nematic/isotropic change was seen. During heating, CNTs bundles turn to isotropic state lastly because the extraordinary fast heat dissipation rate. In contrast, the CNTs agglomerations act as nucleation centres during cooling.

In terms of dispersion effectiveness, sonication time, prior stirring, sonication temperature and CNTs concentrations were reviewed. The size of the CNTs in the LC/MWCNTs composite depends on the sonication time. Combined the naked eyes and microscope observations, the 30 mins sample is the best. However, longer mechanical energy does not necessarily result in fine CNTs bundles. The 5 mins sample is the best in the 24hours prior stirring study. Stirring provide enough energy for dispersion and prolonged sonication induces colloid aggregation by shear flow. For sonication temperature, it is advantageous to keep LC in its nematic state. In the LC self orientated state, the entropy loss due to adsorption induced alignment is negligible and it is favorable for mixing as the free energy is minimized. In addition, the ordered structure resists the formation of CNTs clusters and provides long lasting dispersion stability. The difference of nematic to isotropic transition temperature (T_{NI}) with

different CNTs concentrations can be explained by the two nucleation mechanisms. When CNTs content is high and clusters formed, heterogeneous nucleation will take place. Whereas, homogeneous nucleation will occur and supercooling is needed to initiate nucleation when CNTs content is low. Thus, T_{NI} of high CNTs content composite is lower than pure LC during cooling.

When it comes to EO performance, low CNTs concentration composite improved the threshold voltage and response time. The smallest threshold voltage obtained in the 0.02wt% sample and the fastest response time recorded in the 0.05wt% sample. The decrease in threshold voltage was attributed to the increase in dielectric anisotropy due to the extreme high aspect ratio of the CNTs. The improvement in response time was because of the suppression of the backflow effect and the decrease in rotational viscosity. The reduced rotational viscosity can also be explained by the difference in dielectric anisotropy and aspect ratio of the neat and doped material. When CNTs concentration is high, ion concentration in the system is also high and eventually degraded the display performance. High ion concentration weakens the effective electric field applied on the display and caused image sticking problem. CNTs aggregation is large when CNTs content is high too. This creates light leakage problem and further degrades the display performance.

Overall, there are surely optimized parameters for LC/CNTs dispersion. When we try to enhance the EO performance, comprehensive considerations are needed because improvement in EO performance may reduce the system's stability. By reviewing the studies done by other researchers, the optimization is sensitive to the features of materials. Even the same source of CNTs used but different in outer diameter may result in a completely inconsistent findings. This study only gave an outline on how to optimize the dispersion and EO performance. In fact, the dispersion effectiveness, stability and EO performance is strongly depends on the LC/CNTs matching. In the future, it is worth to put more efforts into the different types of LC materials and CNTs and try to categorize them with the optimal dispersion parameters and CNTs concentration for best EO performance.

References

1. E. Lueder, “Liquid Crystal Displays: Addressing Schemes and Electro-Optical Effects” John Wiley & Sons, New York (2001)
2. J. Gurski & M. Q. Lee, Lyticawhitepaper, (2005)
3. DisplaySearch, “Global TV Shipment Growth Improves to 15% Y/Y in Q4’10 as LCD Share Surges” (2011)
4. H. Yu & W. Lee, Appl. Phys. Lett. 90, 033510 (2007)
5. W. Lee, C. Y. Wang & Y. C. Shih, Appl. Phys. Lett. 85, 513 (2004)
6. C. Y. Huang, C. Y. Hu, H. C. Pan & K. Y. Lo, Jpn. J. Appl. Phys. 44, 8077-8081 (2005)
7. C. Y. Huang, H. C. Pan & C. T. Hsieh, Jpn. J. Appl. Phys. 45, 6392-6394 (2006)
8. S. Y. Jeon, S. H. Shin, J. H. Lee, S. H. Lee & Y. H. Lee, Jpn. J. Appl. Phys. 46, 7801-7802 (2007)
9. W. Lee, J. S. Gau & H. Y. Chen, Appl. Phys. B 81, 171-175 (2005)
10. I. S. Baik, S. Y. Jeon, S. H. Lee, K. A. Park, S. H. Jeong, K. H. An & Y. H. Lee, Appl. Phys. Lett. 87, 263110 (2005)
11. H. Y. Chen & W. Lee, Appl. Phys. Lett. 88, 222105 (2006)
12. P. J. F. Harris, “Carbon Nanotubes and Related Structures, Cambridge University Press”, Cambridge, (1999)
13. R. Saito, G. Dresselhaus & M. S. Dresselhaus, “Physical Properties of Carbon Nanotubes”, Imperial College Press, London, (2001)
14. C. N. R. Rao, B. C. Tatishkumar, A. Govindaraj & M. Nath, ChemPhysChem 2, 78 (2001)
15. E. T. Thostenson, Z. Ren & T. W. Chou, Compos. Sci. Technol. 61, 1899 (2001)
16. R. H. Baughman, A. A. Zakhidov & W. A. de Heer, Science 297, 787 (2002)
17. S. J. Tans, A. R. M. Verschueren & C. Dekker, Nature (London) 393, 49 (1998)
18. P. Avouris, T. Hertel, R. Martel, T. Schmidt, H. R. Shea & R. E. Walkup, Appl. Surf. Sci. 141, 201 (1999)
19. C. Thelander & L. Samuelson, Nanotechnology 13, 108 (2002)
20. G. Torre, W. Blau & T. Torres, Nanotechnology 14, 765 (2003)
21. S. K. Park, S. H. Kim & J. T. Hwang , J. Appl. Polym. Sci 109, 388 (2008)
22. S. Schymura, M. Kühnast, V. Lutz, S. Jagiella, U.D. Weglikowska, S. Roth, F. Giesselmann, C. Tschierske, G. Scalia & J. Lagerwall, Adv. Funct. Mater. 20, 3350-3357 (2010)
23. P.M. Ajayan, L.S. Schadler & P.V. Braun, “Nanocomposite science and technology”. Wiley (2003)
24. F. Reinitzer, Monatshefte für Chemie 9, 421-441 (1888)
25. O. Lehmann, Zeitschrift für Physikalische Chemie 4, 462–72 (1889)
26. T. J. Sluckin, D. A. Dunmur & H. Stegemeyer, “Crystals that Flow”. Taylor and Francis (2004)
27. H. Kelker & B. Scheurle, Angew. Chem. Int. Ed. 8, 884 (1969)
28. G. W. Gray, K. J. Harrison & J. A. Nash , Electronics Lett. 9, 130 (1973).
29. Sergey V. Pasechnik, Vadimir G. Chigrinov & Dina V. Shmeliova, “Liquid Crystals: Viscous and Elastic Properties”, Wiley-VCH Verlag GmbH & Co. KGaA (2009)
30. P. Yeh & C. Gu, “Optics of liquid crystal displays”, 2nd ed, John Wiley & Sons, New York (2010)
31. S. Chandrasekhar, “Liquid Crystals”, 2nd ed., Cambridge: Cambridge University Press (1992)

32. S. T. Wu & C. S. Wu, Phys. Rev.A 42, 2219-2228 (1990)
33. A. D. McNaught & A. Wilkinson, “Compendium of Chemical Terminology (commonly called The Gold Book)”, IUPAC. ISBN 0-86542-684-8 (2007)
34. C. W. Oseen, Trans. Faraday Soc. 29, 883 (1933)
35. F. C. Frank, Disc. Faraday Soc. 25, 19 (1958)
36. "Handbook of Chemistry and Physics", 91st edition, CRC Press, 2010-2011
37. http://www.microtipsusa.com/
38. http://www.sharp.co.uk/cps/rde/xchg/gb/hs.xsl/-/html/lcd-tv.htm
39. H. George, C. Joseph & Z. Louis, Molecular Crystals 8, 293 (1969)
40. G. H. Heilmeier, L. A. Zanoni, & L. A. Barton Proc. IEEE 56, 1162–1171 (1968)
41. Gerhard H. Buntz (Patent Attorney, European Patent Attorney, Physicist, Basel), Information No. 118, issued by Internationale Treuhand AG, Basel, Genf, Zurich. (2005)
42. T. Scheffer & J. Nehring, Appl. Phys. Lett. 45, 1021 (1984)
43. P. J. Bos, P. A. Johnson, Jr. & K. R. Koeler-Beron, SID Symp. Dig. 1983, 30 (1983)
44. M. Oh-e & K. Kondo, Liq. Cryst. 22, 379 (1997)
45. D. S. Seo & J. H. Lee, Jpn. J. Appl. Phys., Part 2 38, L1432 (1999)
46. A. Kubono, Y. Kyokane, Y. Kasajima, R. Akiyama & K. Tanaka, J. Appl. Phys. 89, 3554 (2001)
47. Jaeger, C. Richard, “Lithography”. Introduction to Microelectronic Fabrication. Upper Saddle River: Prentice Hall ISBN 0-201-44494-7 (2002)
48. R. Behrisch, “Sputtering by Particle bombardment”, Springer, Berlin (1981)
49. S. Iijima, Nature (London) 354, 56 (1991)
50. A. Thess, R. Lee, P. Nikdaev, H. Dai, P. Petit, J. Robert, C. Xu, Y. H. Lee, S. G. Kim, A. G. Rinzler, D. T. Colbert, G. E. Scuseria, D. Tomanek, J. E. Fischer & R. E. Smalley, Science 273, 483 (1996)
51. M. Endo, K. Takeuchi, S. Igarashi, K. Kobori, M. Shiraishi, & H. W. Kroto, J. Phys. Chem. Solids 54, 1841 (1993)
52. X. Wang, Q. Li, J. Xie, Z. Jin, J. Wang, Y. Li, K. Jiang & S. Fan, Nano Letters 9, 3137–3141 (2009)
53. M. F. Yu, O. D. Lourie, J. Mark, K. Moloni, K. F. Thomas & R. S. Rodney, Science 287, 637–640 (2000)
54. B. Peng, M. Locascio, P. Zapol, S. Li, S. L. Mielke, G. C. Schatz, & H. D. Espinosa, Nature Nanotechnology 3, 626-631 (2008)
55. S. Hong & S. Myung, Nature Nanotechnology 2, 207–208 (2007)
56. W.A de Heer, A.Chatelain & D.Ugrate, Science 270, 1179 (1995)
57. P.G.Collins & A.Zettl, Appl. Phys. Lett. 69, 1969 (1996)
58. P.G.Collins, K.Bradle y, M.Ishigami & A.Zettl, Science 287, 1801 (2000)
59. J.K.N.Franklin, C.Chou, S.P an, K.J.Cho & H.Dai, Science 287, 622 (2000)
60. A.M.Fennimore, T.D.Y uzvinsky, W.-Q.Han, M.S.Fuhrer, J. Cumings & A.Zettl, Nature 424, 408 (2003)
61. I. Dierking, G. Scalia & P. Morales, J. Appl. Phys. 97, 044309 (2005)
62. I. Dierking, G. Scalia, P. Morales & D. LeClere, Adv. Mat. 16, 865-869 (2004)
63. L. S. Li & J. Y. Huang, J. Phys. D: Appl. Phys. 42, 125413 (2009)
64. M. Copic, A. Mertelj, O. Buchnev & Y. Reznikov, Phys. Rev. E 76, 011702 (2007)

65. S. Kobayashi, T. Miyama, N. Nishida, Y. Sakai, H. Shiraki, Y. Shiraishi & N. Toshima, J. Display Technol 2, 121-129 (2006)
66. H. Yoshikawa, K. Maeda, Y. Shiraishi, J. Xu, H. Shiraki, N. Toshima & S. Kobayashi, Jpn. J. Appl. Phys 41, 1315-1317 (2002)
67. S. Sono, T. Miyama, K. Takatoh & S. Kobayashi, Proc. SPIE–Int. Soc. Opt. Eng. 6135, 1 (2006)
68. F. Haraguchi, K. Inoue, N. Toshima, S. Kobayashi & K. Takatoh, Jpn. J. Appl. Phys. 46, 796–797 (2007)
69. K. J. Wu, K. C. Chu, C. Y Chao, Y. F. Chen, C. W. Lai, C. C. Kang, C. Y. Chen & P. T. Chou, Nano Letters, 7, 1908-1913 (2007)
70. S. M. Huang, L. M. Dai & A. W. H. Mau, J. Phys. Chem. B 103, 4223-4227 (1999)
71. Y. Murakami, S. Chiashi, Y. Miyauchi, M. Hu, M. Ogura, T. Okubo & S. Maruyama, Chem. Phys. Lett. 385, 298-303 (2004)
72. S. Huang, X. Cai, J. Liu & J. Am. Chem. Soc. 125, 5636-5637 (2003)
73. K. Bubke, H. Gnewuch, M. Hempstead, J. Hammer & M. L. H. Green, Appl. Phys. Lett. 71, 1906-1908 (1997)
74. X. Q. Chen, T. Saito, H. Yamada & K. Matsushige, Appl. Phys. Lett. 78, 3714-3716 (2001)
75. D. A. Walters, M. J. Casavant, X. C. Qin, C. B. Huffman, P. J. Boul, L. M. Ericson, E. H. Haroz, M. J. O'Connell, K. Smith, D. T. Colbert & R. E. Smalley, Chem. Phys. Lett. 338, 14-20 (2001)
76. J. E. Fischer, W. Zhou, J. Vavro, M. C. Llaguno, C. Guthy, R. Haggenmueller, M. J. Casavant, D. E. Walters & R. E. Smalley, J. Appl. Phys. 93, 2157-2163 (2003)
77. M.Bockrath, J.Hone, A.Zettl, P.L.McEuen, A.G.Rinzler & R.E.Smalle y, Phys. Rev. B 61, 10606 (2000)
78. S.J.T ans, A.R.M.V erschueren & C.Dekk er, Nature 393, 49 (1998)
79. S. J.Jeong, P. Sureshkumar, K. U. Jeong, A. K. Srivastava, S. H. Lee, S. H. Jeong, Y. H. Lee, R. Lu & S. T. Wu, Opt. Express 15, 11698 (2007)
80. C. Y. Huang, C. H. Pan & C. T. Hsieh, Japan. J. Appl. Phys. 45, 6392 (2006)
81. S. Zhang, I. A. Kinloch & A. Windle, Nano. Lett. 6, 568 (2006)
82. O. Trushkevych et al, J. Phys. D: Appl. Phys. 41, 125106 (2008)
83. S. K. Park, S. H. Kim & J. T. Hwang, J. Appl. Polym. Sci. 109, 388 (2008)
84. J. L Bahr, J. Yang, D. V. Kosynkin, M. J. Bronikowski, R. E. Smalley & J. M. Tour, J. Am. Chem. Soc. 123, 6536 (2001)
85. C. Y Huang, Y. G Lin & Y. J Huang, Jpn. J. Appl. Phys. 47 (2008) pp. 6407-6409
86. W. H. Song & Alan H. Windle, Macromoolecules, 38, 6181-6188 (2005)
87. Jan P. F. Lagerwall & G. Scalia, J.Mater. Chem., 18, 2890-2898 (2008)
88. M.S. Dresselhaus, G. Dresselhaus, A. Jorio, A.G. Souza Filho, R. Saito, Carbon, 40, 2043 (2002)
89. J.M.C. Moreno, M. Yoshimura, J. Am. Chem. Soc., 123, 741 (2001)
90. J.-Y. Chang, A. Ghule, J.-J. Chang, S.-H. Tzing, Y.-C. Ling, Chem. Phys. Lett., 363, 583 (2002)
91. P C Eklund, J M Holden, R A Jishi, Carbon, 33, 7, 959-972 (1995)
92. http://wcm.ustc.edu.cn/pub/est_ustc/szdw_1/fjs/201109/P020130114595528099208.pdf
93. M. Grujicic , G. Cao , W. N. Roy , J. Mater. Sci., 39, 2315 (2004)
94. M. Sano , T. Kunitake , Langmuir, 8 , 320 (1992)